NUREG/CR-5314
EGG-2562
Vol. 3

Life Assessment Procedures for Major LWR Components

Cast Stainless Steel Components

Prepared by C. E. Jaske, V. N. Shah

Idaho National Engineering Laboratory
EG&G Idaho, Inc.

Prepared for
U.S. Nuclear Regulatory Commission

AVAILABILITY NOTICE

Availability of Reference Materials Cited in NRC Publications

Most documents cited in NRC publications will be available from one of the following sources:

1. The NRC Public Document Room, 2120 L Street, NW, Lower Level, Washington, DC 20555
2. The Superintendent of Documents, U.S. Government Printing Office, P.O. Box 37082, Washington, DC 20013-7082
3. The National Technical Information Service, Springfield, VA 22161

Although the listing that follows represents the majority of documents cited in NRC publications, it is not intended to be exhaustive.

Referenced documents available for inspection and copying for a fee from the NRC Public Document Room include NRC correspondence and internal NRC memoranda; NRC Office of Inspection and Enforcement bulletins, circulars, information notices, inspection and investigation notices; Licensee Event Reports; vendor reports and correspondence; Commission papers; and applicant and licensee documents and correspondence.

The following documents in the NUREG series are available for purchase from the GPO Sales Program: formal NRC staff and contractor reports, NRC-sponsored conference proceedings, and NRC booklets and brochures. Also available are Regulatory Guides, NRC regulations in the *Code of Federal Regulations*, and *Nuclear Regulatory Commission Issuances*.

Documents available from the National Technical Information Service include NUREG series reports and technical reports prepared by other federal agencies and reports prepared by the Atomic Energy Commission, forerunner agency to the Nuclear Regulatory Commission.

Documents available from public and special technical libraries include all open literature items, such as books, journal and periodical articles, and transactions. *Federal Register* notices, federal and state legislation, and congressional reports can usually be obtained from these libraries.

Documents such as theses, dissertations, foreign reports and translations, and non-NRC conference proceedings are available for purchase from the organization sponsoring the publication cited.

Single copies of NRC draft reports are available free, to the extent of supply, upon written request to the Office of Information Resources Management, Distribution Section, U.S. Nuclear Regulatory Commission, Washington, DC 20555.

Copies of industry codes and standards used in a substantive manner in the NRC regulatory process are maintained at the NRC Library, 7920 Norfolk Avenue, Bethesda, Maryland, and are available there for reference use by the public. Codes and standards are usually copyrighted and may be purchased from the originating organization or, if they are American National Standards, from the American National Standards Institute, 1430 Broadway, New York, NY 10018.

DISCLAIMER NOTICE

NUREG/CR-5314
EGG-2562
Vol. 3
RM, R9

Life Assessment Procedures for Major LWR Components

Cast Stainless Steel Components

Manuscript Completed: September 1990
Date Published: October 1990

Prepared by
C. E. Jaske, V. N. Shah

G. H. Weidenhamer, NRC Program Manager

Idaho National Engineering Laboratory
Managed by the U.S. Department of Energy

EG&G Idaho, Inc.
Idaho Falls, ID 83415

Prepared for
Division of Engineering
Office of Nuclear Regulatory Research
U.S. Nuclear Regulatory Commission
Washington, DC 20555
NRC FIN A6389
Under DOE Contract No. DE-AC07-76ID01570

ABSTRACT

This report presents a procedure for estimating the current condition and residual life of safety–related cast stainless steel components in light water reactors (LWRs). The procedure accounts for loss of fracture toughness caused by thermal embrittlement and includes the following: a review of design and fabrication records, inservice inspection records, and operating history; a fracture mechanics evaluation to determine the required toughness at end–of–life using worst–loads and worst–flaw indications; current and future toughness estimates; and criteria regarding continued service, repair, or replacement of the component being evaluated. The report discusses the available Charpy V–notch impact energy, fracture toughness, tensile strength, fatigue resistance, and fatigue–crack growth data, and presents two methods for assessing the degree of thermal embrittlement: metallurgical evaluation and analytical modeling of inservice degradation.

INEL FOREWORD

The United States was one of the first nations to use nuclear power to commercially generate electricity and, therefore, has some of the oldest operating commercial reactors. As U.S. light water reactors (LWRs) have matured, problems associated with time– or use–dependent degradation (aging) mechanisms such as stress corrosion, radiation embrittlement, fatigue, and other effects have occurred and have raised questions about the continued safety and viability of older nuclear plants. Some of the recent aging–related problems include primary water stress corrosion cracking of pressurized water reactor (PWR) pressurizer heater sleeves and instrument nozzles and PWR steam generator tube plugs, steam generator tube ruptures caused by high–cycle fatigue and by a failed tube plug, significant wall–thinning of light water reactor metal containments caused by corrosion, fatigue failure of boiling water reactor (BWR) recirculation pump internals (resulting in potential damage to reactor pressure vessel core and internals), catastrophic failure of a "nonnuclear" portion of a PWR feedwater line caused by erosion–corrosion, and through–wall thermal–fatigue cracks in high–pressure safety injection lines and a residual heat removal line.

At the same time, with a continually increasing demand for electricity and limited new generating capacity under construction, the U.S. electric utilities are motivated to keep their existing plants operating beyond the original design life at as high a capacity as possible. The economics of plant life extension are clearly favorable. Studies cosponsored by the U.S. Department of Energy (DOE) and the Electric Power Research Institute (EPRI) show that replacing any single nuclear plant component can easily be justified, if the life of the plant can be extended for a number of years. Extending the life of a 1000–MW plant by 20 years is expected to realize a net present worth of perhaps $1 billion.

Therefore, the potential problems of managing aging in older plants and the resolution of technical safety issues in consideration of the development of appropriate license renewal criteria have become a major focus for the research sponsored by the U.S. Nuclear Regulatory Commission (USNRC). An important part of the USNRC research effort is the Nuclear Plant Aging Research (NPAR) Program that is being conducted at several national laboratories, including the Idaho National Engineering Laboratory (INEL). One of the NPAR program tasks at the INEL is to develop the appropriate technical criteria for the USNRC to assess the residual life of the major PWR and BWR components and structures. These assessments will help the USNRC identify and resolve safety issues associated with LWR aging degradation and develop policies and guidelines for making operating plant license renewal decisions.

Most of the effort for this life assessment task is focused on integrating, evaluating, and updating the technical information relevant to aging and license renewal from current or completed NRC and industry research programs. A five–step approach is being pursued to accomplish the life assessment task: (1) identify and prioritize major components, (2) identify degradation sites, mechanisms and stressors, and potential failure modes for each component, and then evaluate the current inservice inspection (ISI) methods, (3) assess advanced inspection, surveillance, and monitoring methods, (4) develop life assessment models and procedures, and (5) support the development of technical criteria for license renewal.

A brief discussion of each of these steps follows:

1. *Identification and prioritization of major components*: Virtually all major equipment contained within a nuclear plant complex is subject to some aging degradation and must be evaluated in an aging and licensee renewal program. From the USNRC's perspective of ensuring the health and safety of the public, the first step in this assessment task was to identify those major components critical to nuclear power plant safety. Components that help contain the release of fission products during normal, off–normal, or accident conditions were selected. The PWR components (in rough order of importance) include the reactor pressure vessel (RPV); the containment and basemat; reactor primary coolant piping, safe ends, and nozzles; steam generators; reactor coolant pump bodies; pressurizer and associated surge and spray lines; control rod drive mechanisms; cables and connectors; emergency diesel generators; RPV internals; RPV supports; and feedwater lines and nozzles. A similar list was developed for BWRs except that the containment was ranked most important. Although some PWR steam generator and BWR recirculation piping have been replaced, their replacement is a major, time–consuming operation. In addition, steam generator tubes and recirculation piping constitute a part of the primary pressure boundary, and therefore, aging

evaluation of these components is included in this task. The lifetime of many of the smaller, less expensive components such as the pumps, valves, sensors, batteries, controls, etc. is often less then the initial license period of 40 years, and these components are usually repaired, refurbished, or replaced relatively frequently. Therefore, these components are being studied in other NPAR tasks that are focusing more on reliability, availability, and maintainability than on life assessments.

2. *Identification of the degradation sites, mechanisms and stressors, and the potential failure modes and evaluation of the current ISI methods*: Time–or use–dependent damage or aging can be caused by one or several different mechanisms active within a component, structure, or material and, if not recognized and properly managed, may result in some type of failure or impairment of function. The degradation is often the result of interactions between design, materials, operational stressors, and environments. Poor design, improper material selection, severe environments, or inadequate maintenance practices can accelerate the degradation. Therefore, identification and understanding of the design, materials, stressors, environments, and aging mechanisms is essential. This step consists of identifying and qualitatively evaluating the stressors, potential degradation sites and mechanisms, probable failure modes, and current ISI methods for each of the selected major components. This qualitative analysis of the degradation sites and processes and current ISI methods is essential to developing a proper understanding of the impact of aging on safe operation of nuclear power plants and identifying and prioritizing the unresolved technical issues relevant to nuclear power plant aging and license renewal.

3. *Assessment of advanced inspection, surveillance, and monitoring methods*: Knowledge of the current damage state of the material is essential for a proper assessment of the residual life of a component or structure. Inservice inspections are performed to measure the current state of damage. However, many of the standard nondestructive examination (NDE) methods employed to satisfy current ISI requirements were developed for the detection and qualitative assessment of fabrication–related flaws. These methods are not entirely adequate for residual life assessment. Inspections for life assessment generally require greater detection reliability and a more quantitative determination of defects and accumulated damage than traditional ISI. Therefore, it is essential that emerging methods for inspection be developed and evaluated and that they accurately determine, for example, the size, shape, location, orientation, and type of both surface and internal flaws.

4. *Develop (or evaluate) life assessment models and procedures*: An important feature of this NPAR task is the development of models or procedures to estimate the remaining useful life of the major, risk–significant LWR components and structures. The residual life assessment models and procedures appropriate for various structures and components may differ considerably. However, a general approach that may work well for many of the reactor primary system pressure boundary components, the containment, and possibly other major components is as follows: (a) evaluate the present state of the component, (b) estimate the change expected during the planned operating period, (c) identify appropriate design requirements, and (d) compare the estimated condition of the component at the end of the planned operating period with the design requirements.

   The component state or condition of interest might be one or more of its material properties, such as fracture toughness, fatigue usage, strength, elasticity, etc., and/or one or more geometry characteristics, such as flaw size, wall thinning from wear, corrosion, and erosion, tolerances, etc. These characteristics can be determined by inspection, destructive examination, analysis, or other methods. However, note that the use of analysis to estimate key material properties (such as fracture toughness or elasticity) and component geometry changes from wear, corrosion, erosion, flaw growth, etc., generally requires a good knowledge of the initial material condition and tolerances and a very good understanding of the relationships between stressors and states. This understanding must be based on appropriate data and physical models.

   The changes in the component state or condition during some future planned operating period (such as a license renewal period) can be

estimated based on conservative extrapolation of previous ISI (for example, wall thickness data) and destructive examination measurements or analysis. Again, the analysis tools should reflect a good understanding of the physical relationships between the operating stressors and the changes in the component state or condition.

The component or structural design requirements should be based on traditional engineering analyses (thermal, hydraulic, stress, neutronic, etc., as appropriate) or testing and reflect appropriate margins between the expected loads and the calculated failure loads. The original design analysis may be sufficient for some components. A revised design analysis may be necessary for other components subject to additional cycles, previously unknown stressors, etc. New information may, in some cases, allow a reduction in or revised estimate of the margin.

The final step, comparing the design requirements with the expected condition of the component, would be followed, of course, by a decision to replace or repair the component or leave the component as is. The comparison of design requirements with a component's expected condition might also influence the planned future operating period (license renewal period) and the frequency of future ISI or destructive examination activities.

A somewhat different approach is associated with components subject to environmental qualification (EQ) requirements. These are components that must function properly during a normal operating period of some given duration and also during selected design basis accidents (DBA). Here three general approaches might be considered: (a) compare actual operating environments with the preaging EQ environments, (b) compare estimated mechanical properties at the end of the planned operating period with the preaged EQ sample mechanical properties, and (c) remove samples from the plant, add additional aging (to reflect the expected aging during the planned future operating period), and subject the samples to DBA testing. The first two approaches require modeling of the complex relationships between environmental stressors, aging degradation (which are often material property changes), and time. The third approach provides results with more certainty but possibly at the highest cost.

The residual life assessment models or procedures will have a strong impact on the development of technical criteria for license renewal. It is important that the limitations and uncertainties associated with whichever approach is chosen be assessed so that confidence intervals can be calculated and safety margins properly assessed.

5. *Development of technical criteria for license renewal*: The results and outputs obtained from the activities discussed above will be used to help the USNRC identify and resolve technical safety issues associated with LWR aging degradation and develop policies and guidelines for making license renewal decisions. The qualitative analysis of the degradation sites and processes and current ISI methods (Step 2) will facilitate the identification and prioritization of the unresolved technical issues relevant to nuclear power plant aging and license renewal. The qualitative analysis will also help provide the USNRC and industry a basis for life assessment model (or procedure) development. The assessments of the advanced inspection, surveillance and monitoring methods could provide a technical basis for acceptance or rejection of any ISI associated with a life assessment. Most important, the use of acceptable life assessment models or procedures could form the technical basis for a revised license renewal safety analysis report (SAR) as well as a revised NRC standard review plan and regulatory guides.

Overall project results to date are as follows. The first two steps have been completed, and results are presented in a two-volume report: *Residual Life Assessment of Major Light Water Reactor Components – Overview*, NUREG/CR-4731. Some progress has been made on Step 3, the assessment of emerging inspection, surveillance, and monitoring methods. The emerging inspection, monitoring, and material evaluation methods are briefly discussed in Volume 1 of NUREG/CR-4731. An indepth assessment of both advanced fatigue monitoring and material evaluation methods will be published in the near future. Indepth assessments of improved acoustic monitoring, advanced ultrasonic testing, and eddy current techniques are in progress.

Life assessment procedures will be published soon for five major components as part of Step 4: PWR

reactor pressure vessels, reinforced concrete containments, cast stainless steel components, PWR steam generator tubes, and metal containments. We plan to publish these procedures in this multi-volume NUREG report, as indicated below.

PWR Reactor Pressure Vessels – Volume 1
Reinforced Concrete Containments – Volume 2
Cast Stainless Steel Components – Volume 3
PWR Steam Generator Tubes – Volume 4
Metal Containments – Volume 5

Life assessment models or procedures for the other major components and structures will be presented in future volumes of this report.

P. E. MacDonald
V. N. Shah
September 1990

EXECUTIVE SUMMARY

Many critical pressure boundary components in commercial light water reactors (LWRs) are composed of cast stainless steels. Life assessment procedures are needed for these components because cast stainless steels are subject to thermal embrittlement during long-term service exposure at LWR operating temperatures. The components of concern include pump bodies, reactor coolant piping and fittings, surge lines (in a few plants), pressurizer spray heads, check valves, control rod drive mechanism housings, and control rod assembly housings. These are made of grade CF-8, CF-8A, or CF-8M stainless steel in U.S. LWRs; grade CF-3 stainless steel also is used in some foreign LWRs. The purpose of this project was to review the available data on thermal embrittlement of cast stainless steels and to develop updated procedures for life assessment of key LWR cast stainless steel components.

Cast stainless steels have a two-phase microstructure consisting of ferrite islands in an austenite matrix. With long-term thermal exposure at LWR operating temperatures, other phases form in the ferrite phase that cause it to become hard and brittle, while the austenite remains ductile. If the amount of ferrite is small, and if it is distributed evenly and finely throughout the austenite, then the properties of the casting are not significantly affected by the thermal embrittlement of the ferrite. However, as the amount of ferrite and the coarseness of its distribution increase, the thermal embrittlement of the ferrite increasingly affects the properties of the casting.

The properties most affected by thermal embrittlement are Charpy V-notch (CVN) impact energy and fracture toughness (J_{Ic}). Both of these properties decrease as the degree of thermal embrittlement increases. If these values become too low, the structural integrity of a cast stainless steel component could be seriously impaired. The available data indicate that thermal embrittlement does not have a large effect on tensile, fatigue-crack initiation, or low-cycle fatigue-crack growth behavior. However, more fatigue-crack-growth data are needed for CF-8 and for all cast stainless steels in the high-cycle (low growth rate, near threshold) regime. Thus, for life assessment of cast stainless steel components, the main concern is loss of fracture toughness and impact energy. Data and engineering models have been developed to help predict the degree of embrittlement as a function of thermal exposure history. For reactor internals, there also is a concern that irradiation may embrittle the austenite and add to the overall embrittlement of the component. No information on this potential problem was found during this project, but it is an area that merits future study.

The minimum CVN impact energy after long-term aging has been found to be proportional to the square of the fraction of ferrite, the mean ferrite spacing, and a chemical-composition parameter. This model should be developed further for application to the assessment of components. A time-temperature parameter can be used to define lower-bound trends to the available impact energy values for cast stainless steels as a function of chemical composition and thermal exposure time. In this project we propose a model that uses that parameter to predict the impact energy decrease for any particular lot of cast stainless steel. This predicted impact energy value or the predicted minimum impact energy value is then used to estimate fracture toughness from correlations between impact energy and fracture toughness at both room temperature and 290°C. This proposed approach should provide a conservative estimate of fracture toughness for use in the structural integrity assessment of cast stainless steel components.

Inservice inspection (ISI) is needed to define type, size, and location of defects in cast stainless steel components so that the structural integrity of these components can be evaluated. Use of radiography during ISI is less practical than during fabrication and is inefficient. In addition, conventional ultrasonic testing (UT) methods are not reliable to detect flaws in cast stainless steel components because coarse grains and different grain structures in cast stainless steel result in a low signal-to-noise ratio. Advanced UT methods with enhanced signal-to-noise ratios are being developed. These methods have an improved capability to detect flaws in cast stainless steel components and have been used to inspect statically cast components in several PWR plants. The effect of grain structure on the propagation of ultrasonic waves in cast stainless steel material has been studied to increase the accuracy of locating defects. Because of the difficulties with radiography and UT methods to detect and size flaws, application of the acoustic emission technique to detect crack growth in cast stainless steel needs to be evaluated.

Weld repair procedures are employed to remove fabrication defects during the original production of cast stainless steel components. It should be possible to

adapt, modify, and qualify those procedures for performing weld repairs to components that are in service in order to extend their useful life.

We developed a procedure for estimating the current condition and residual life of key LWR cast stainless steel components. The procedure is implemented in nine major steps. The first three steps involve the collection, examination, and storage of records for fabrication and construction, inservice inspection, and operating history. The fourth step involves a conservative fatigue and fracture mechanics evaluation to determine the worst–case flaw size and the minimum required fracture toughness at the end of the next operating period. In the fifth step, the current condition of the material is assessed using either a proposed analytical model, microstructural data, or measured properties (or using some combination of those three methods). In the sixth step, the results of the fourth and fifth steps are combined to evaluate the structural integrity of the component. The seventh step establishes what actions (none, repair, replace, or shut down) are to be taken, and the eighth step establishes the plan for the next ISI. From this point, the steps are repeated (the component is reevaluated) as needed.

Future work is recommended to provide information for use in implementing the life assessment procedure. Guidelines of worst–case thermal embrittlement data should be developed. Thermal embrittlement surveillance programs should be initiated. More impact and fracture toughness data should be developed for material aged and tested at maximum LWR operating temperatures. The aging parameter model should be improved to better account for the observed mechanisms of thermal embrittlement. The work on evaluation of the relation of ferrite amount and spacing to the degree of embrittlement should be continued. High–cycle fatigue–crack–growth tests should be performed on aged and irradiated materials, especially CF–8. The use of field replication and magnetic measurements for characterizing cast stainless steels should be demonstrated and validated. Techniques involving the use of substandard sized specimens and microhardness to quantify the degree of thermal embrittlement should be developed. Repair welding procedures should be qualified and validated. Fracture–mechanics analyses should be performed for representative combinations of components and operating histories to estimate the minimum fracture toughness required for safe operation. ISI methods and programs should be modified to incorporate procedures and evaluations appropriate to cast stainless steel components.

ACKNOWLEDGMENTS

The authors of this report acknowledge the significant role that G. H. Weidenhamer of the U.S. Nuclear Regulatory Commission has played in providing programmatic guidance and review for this report.

The authors sincerely appreciate the critical review of this report performed by B. I. Landerman. The authors thank O. K. Chopra and H. M. Chung of Argonne National Laboratory and M. B. Lapides of Electric Power Research Institute for several telephone conversations and meetings related to aging of cast stainless steel components. The authors also thank O. K. Chopra for providing the data from the Charpy impact tests of aged cast stainless steel specimens, and thank M. B. Lapides for providing a summary of a draft EPRI report on aging of cast stainless steel components. The authors thank C. W. Rainger of Sandusky Foundary & Machine Company for reviewing the report.

Finally, the authors thank D. R. Pack and D. L. Bramwell of the Idaho National Engineering Laboratory for their technical editing assistance and the significant effort they put forth in coordinating the production of this report, and to K. O. Roberts and B. L. Thompson for their special effort in composing the document.

CONTENTS

FIGURES

TABLES

LIFE ASSESSMENT PROCEDURES FOR MAJOR LWR COMPONENTS VOLUME 3: CAST STAINLESS STEEL COMPONENTS

1. INTRODUCTION

All operating commercial nuclear power plants in the United States are light water reactor (LWR) systems; they employ a variety of cast stainless steel components in the primary pressure boundary. Cast stainless steel is used because of its high resistance to hot cracking, corrosion, and stress–corrosion cracking, and because of its improved mechanical properties (Solomon and Devine, Jr., 1983). In addition, use of cast stainless steel provides benefits of the casting process in manufacturing. Complex shapes, such as pump housings, valve bodies, and fittings are statically cast; usually the molten metal is poured into a fixed sand mold. Cylindrical shapes, such as pipes, are centrifugally cast; the molten metal is poured into a rotating sand–lined metal casing.

Maintaining the structural integrity of these components is essential to the safe operation of the power plants. Thus, any mechanism that may degrade the mechanical properties of the cast stainless steels used in these components should be considered in efforts to extend the operating life of an LWR. Thermal embrittlement at LWR operating temperatures is the major degradation mechanism of concern for cast stainless steel components. Typical operating temperatures in pressurized water reactor (PWR) primary coolant piping varies from 288 to 327°C (550 to 621°F) (Shah and MacDonald, 1987), and the PWR pressurizers operate at 343°C (650°F). The typical operating temperature in boiling water reactors is about 282°C (540°F) (Shah and MacDonald, 1989). For service exposure in this relatively low–temperature range, the embrittlement occurs at a very slow rate over a period of many years.

As aging progresses, and the degree of embrittlement increases, the critical flaw size decreases; thus, even initial defects that do not grow, as well as those that may grow subcritically, may in time become defects of critical size. During structural integrity assessments of cast stainless steel components, one must determine if the critical defect size will become too small to be reliably detected during inservice inspection (ISI). Finally, leak–before–break (LBB) analysis should be performed to determine if a detectable leak will develop before a growing crack reaches a critical size for unstable propagation.

The concern about possible thermal embrittlement becomes progressively more important as cast stainless steel components enter the second half of the 40–yr period of a nuclear power plant's original operating license, and as extending the operating license for an additional period of 20 years or more is considered. The potential problem of thermal embrittlement is aggravated by the fact that the current nondestructive examination (NDE) techniques used for wrought stainless steels usually are not as effective when applied to cast stainless steels.

The objectives of this report are to review the available information on thermal embrittlement of cast stainless steels, discuss methods of assessing the degree of embrittlement for inservice cast stainless steel components, discuss the possible effects of inservice repair welding on thermal embrittlement, and suggest possible approaches for evaluating the remaining safe life of cast stainless steel components, approaches that can be used in efforts to extend the operating license of a light water reactor. To provide background for these discussions, the following sections of this introduction briefly describe (a) the LWR cast stainless steel components of interest and (b) the physical metallurgy of cast stainless steels.

1.1 LWR Cast Stainless Steel Components

Table 1 lists the eight LWR cast stainless steel components considered in this project. The following paragraphs give brief descriptions of these components.

Reactor Coolant Pump Body. Three types of reactor coolant pump bodies are used in LWR plants. Types F and E pumps are used in PWRs, and Type C pumps are used in BWRs. Pump bodies are manufactured using CF–8, CF–8A, or CF–8M statically cast stainless steel sections that are subsequently welded. The casting is typically done in more than one piece because of the

Table 1. LWR cast stainless steel components

Component	Type of Casting	Grade	Number of Plants	Comments
Reactor Coolant Pump Body	Static	CF–8 CF–8M CF–8A		Type F in 61 plants Type E in 15 plants Type C in all BWRs
Coolant Piping	Centrifugal	CF–8A CF–8M	20 7	44% of Westinghouse plants
Coolant Piping Fittings	Static	CF–8A	27	All Westinghouse plants
Surge Lines	Centrifugal	CF–8M		Some Combustion Engineering Plants
Pressurizer Spray Head	Static			Westinghouse plants
Check Valves	Static	CF–8M		Some Westinghouse plants
Recirculation Piping Fittings	Static	CF–8 CF–8M		BWR plants
Control Rod Drive Mechanism Housing	Static	CF–8		Some Westinghouse plants
Core Internals	Static	CF–8, CF–3		PWR and BWR plants

size of the pump body, and the pieces are welded together to produce the final assembly (Shah and MacDonald, 1989). Recent designs of Type F pump casings decreased or eliminated the number of weldments as it became practical to manufacture larger casting sections. The pump impellers are made of CF–8 cast stainless steel. Figures 1 through 3 show the pump configurations (ASME Code Section III).

Figure 1 shows a Type F pump. Most Type F pumps are manufactured by Westinghouse. Their wall thickness ranges from 100 to 200 mm (4 to 8 in.). These pumps are used in Westinghouse and some Babcock & Wilcox (B&W) plants. Type F pumps are used in a total of 61 nuclear plants. The Bingham–Willamette Company also makes Type F pumps that are used in some B&W plants. Type F pumps are manufactured using an electroslag welding process with no postweld heat treatment; the lack of such treatment can leave some high residual stresses at levels near yield strength. (Section III of the ASME Boiler and Pressure Vessel Code for Class I components neither requires nor prohibits postweld heat treatments for austenitic stainless steel welds.)

Figure 2 shows a Type E pump. Type E pumps are manufactured by Byron Jackson Pump Division, Borg–Warner Corporation. These pumps have wall thicknesses in the range of 60 to 80 mm (2 to 3 in.). They are used in 15 B&W and Combustion Engineering (CE) plants. These pumps are manufactured with manual welds followed by a full solution heat treatment, which eliminates nearly all the residual stresses if the assembly is slowly cooled from the solution treating temperature. However, the welded castings are quenched from the solution treatment temperatures [~1038 to 1149°C (1900 to 2100°F)] to avoid sensitization, which can leave high residual stresses (Shah and MacDonald, 1989). Any improvement provided by solution heat treatment is limited because the sections of the pump body are thick. The optimum improvement will be at and near the surface, because the

rate of cooling is important. To minimize sensitization and residual streasses in Type E and C pumps (described in the next paragraph), all welding performed after the solution heat treatment of the material is limited to a low–heat input no greater than 1900 J/cm (5000 J/in.).

Figure 3 shows a Type C pump. Type C pumps are manufactured by Byron Jackson Pump Division, Borg–Warner Corporation, for use in all GE BWR plants. These are smaller than the pumps used in PWR plants. The smaller size accommodates the lower system pressures and space limitations of BWRs. Type C pumps also are manufactured with manual welds followed by a full solution heat treatment. In most cases, these welded castings also are quenched from the solution treatment temperature, which can leave high residual stresses.

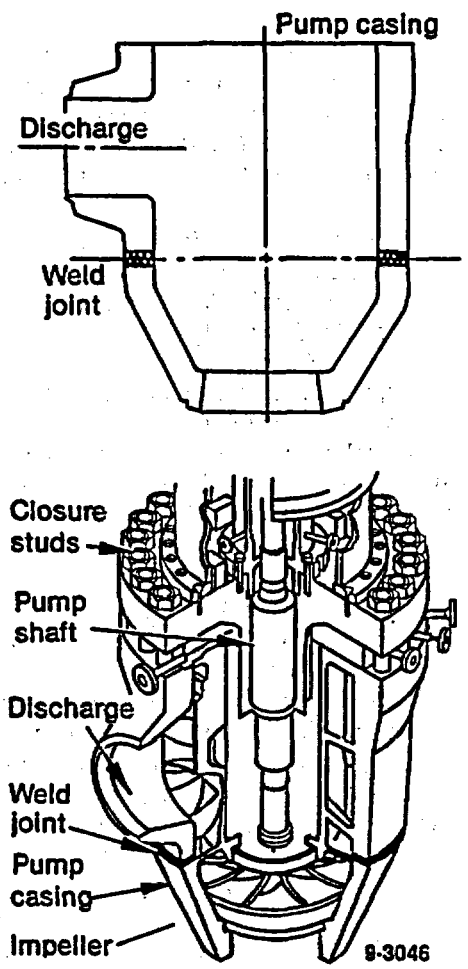

Figure 1. PWR Type F coolant pump.

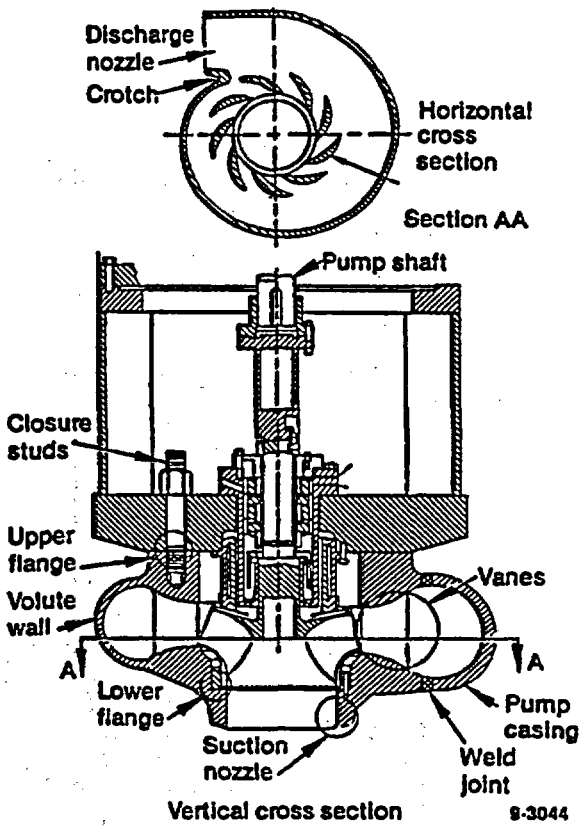

Figure 2. PWR Type E coolant pump.

Reactor Coolant Piping. The newer Westinghouse plants use centrifugally cast CF–8A or CF–8M stainless steel for the main coolant piping (Shah and MacDonald, 1987). CE, B&W, and older Westinghouse plants did not use cast stainless steel for main coolant piping. Table 2 gives the names, sizes, operating age in years, and piping materials for the 27 Westinghouse plants with cast stainless steel primary piping (Egan et al., 1987; USNRC, 1988a). The plants are listed in chronological order of their operating license dates. The typical diameter of the coolant piping is about 0.8 m (32 in.). Almost no problems have been detected in centrifugally cast piping to date (Egan et al., 1987).

Reactor Coolant Piping Fittings. The main coolant piping fittings, such as elbows, are statically cast CF–8A stainless steel. All Westinghouse plants use this material in the primary coolant pipe fittings. Generally, a larger population and deeper defects are expected in statically cast components than in welds or

centrifugally cast components. This should be taken into account when selecting sites for inservice inspections.

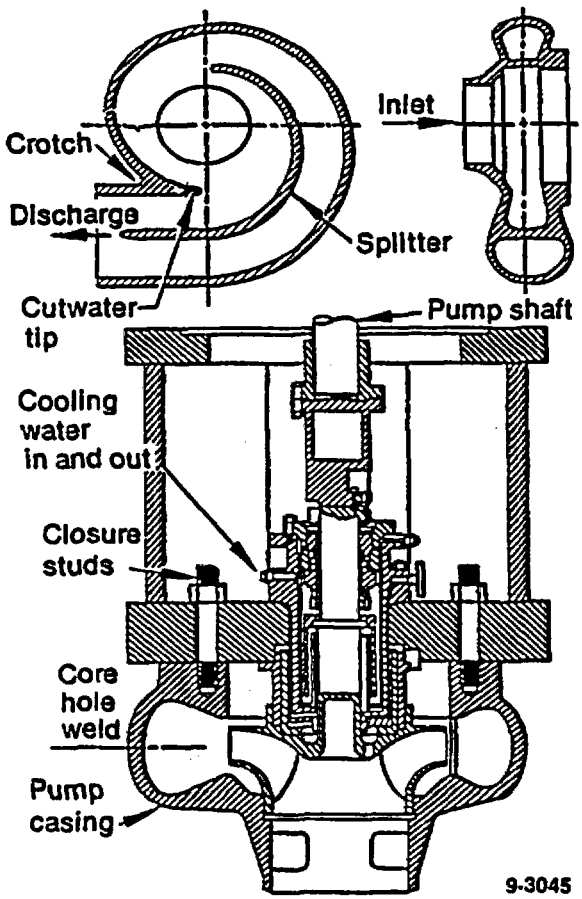

Figure 3. BWR Type C coolant pump.

Surge Line. The surge line connects the reactor coolant piping hot leg to the pressurizer. As the temperature of the reactor coolant fluctuates, the volume increases or decreases, causing water to flow into or out of the pressurizer through the surge line. Typically, the surge line is made of austenitic stainless steel. However, in some Combustion-Engineering plants the surge line is made of CF-8M stainless steel. This line is typically 300-mm (12-in.) diameter Schedule 160 pipe (Shah and MacDonald, 1989). The pressurizer end of the surge line has operating temperatures as high as ~343°C, which is the highest operating temperature of the major PWR primary coolant pressure boundary components.

Pressurizer Spray Head. The pressurizer spray head is the termination of the spray line and is located in the steam space of the pressurizer. The cold-leg coolant sprays through the spray head into the pressurizer to reduce the pressure in the primary coolant system. In Westinghouse plants, the spray head is made of cast stainless steel and is subjected to an operating temperature of approximately 343°C (650°F), which is the saturation temperature at the PWR operating pressure.

Check Valves. Check valves with cast stainless steel bodies are installed in LWR safety systems having stainless steel piping. For example, in Westinghouse emergency core cooling systems (ECCS), there are cast stainless steel check valves to prevent flow from the primary loop hot leg or cold leg back into the ECCS piping (USNRC, 1988b; Greenstreet et al., 1985).

Recirculation Piping Fittings and Valves. The BWR recirculation piping fittings, such as elbows and tees, and pump suction and discharge valves, are statically cast CF-8 and CF-8M stainless steel.

Control Rod Drive Mechanism Housing. The control rod drive mechanism (CRDM) housing constitutes a primary pressure boundary. In certain Westinghouse plants, some of the CRDM housings are made of CF-8 cast stainless steel (Shah and MacDonald, 1989).

Core Internals. Core internals made of cast stainless steel may be subjected to both thermal and irradiation embrittlement during long-term service. In CE plants, the control rod assembly shrouds are made of centrifugally cast CF-8 stainless steel. In Westinghouse-type plants, the lower support structures, cruciform instruments guides, and flow mixer plates are made of stainless steel castings. In GE plants, the orificed fuel supports are made of CF-8, and parts of the jet-pump assembly are made of CF-8 and CF-3 stainless steel castings.

An evaluation of the effects of irradiation on stainless steel castings should be made. This report reviews the thermal embrittlement of such castings. The thermal embrittlement is caused by embrittlement of the ferrite phase in the ferrite/austenite microstructure that is inherent in these alloys. The austenite phase is ductile and remains so after thermal exposure; thus, when the fraction of ferrite is small, the degree of overall embrittlement of the casting is low. However, if the components used in internals are subjected to high levels of irradiation, the austenite phase could become embrittled as well. In such a case, where both the austenite and ferrite phases are embrittled, the overall structural integrity of the casting could be in question.

Table 2. Cast primary coolant piping materials (Egan et al., 1987; USNRC, 1988a)

Plant Name	Unit Size (MWe)	Number of System Loops	Operating Age[a] (Years)	Pipe Material
Kewaunee	560	2	14	CF–8M
Prairie Island 2	530	2	14	CF–8M
Cook 1	1090	4	12	CF–8M
Farley A	829	3	10	CF–8A
Trojan	1130	4	9	CF–8A
Cook 2	1054	4	9	CF–8M
Beaver Valley 1	852	3	9	CF–8M
North Anna 1	934	3	9	CF–8M
North Anna 2	788	3	8	CF–8A
Farley 2	829	3	8	CF–8A
McGuire 1	1180	4	7	CF–8A
McGuire 2	1180	4	5	CF–8A
Callaway 1	1157	4	5	CF–8A
Sequoyah 1	1140	4	5	CF–8M
Sequoyah 2	1140	4	5	CF–8M
Catawba 1	1153	4	4	CF–8A
Wolf Creek	1158	4	4	CF–8A
Millstone 3	1150	4	4	CF–8A
Catawaba 2	1153	4	3	CF–8A
Vogtle 1	1113	4	3	CF–8A
Beaver Valley 2	852	3	2	CF–8A
South Texas 1	1250	4	2	CF–8A
South Texas 2	1250	4	1	CF–8A
Vogtle 2	1113	4	1	CF–8A
Commanche Peak 1	1150	4	0	CF–8A
Commanche Peak 2	1150	4	0	CF–8A
Watts Bar 1	1177	4	0	CF–8A

a. These values were derived from United States Nuclear Regulatory Commission operating reports (NUREG–0020) for plant service up to May 1990. The values represent the number of years that have elapsed since the operating license dates.

1.2 Physical Metallurgy of Cast Stainless Steels

The required chemical compositions and the required tensile properties of six common grades of cast stainless steel are listed in Tables 3 and 4, respectively. The compositions of CF–3, CF–8, CF–3M, and CF–8M are similar to those of the wrought grades Type 304L, Type 304, Type 316L, and Type 316, respectively. The wrought grades have microstructures that are usually fully austenitic, whereas the cast grades typically have microstructures consisting of about 5 to 25% (volume) ferrite and the balance austenite (Peckner and Bernstein, 1977). (The ferrite phase in cast stainless steels and stainless steel welds is sometimes referred to as the delta ferrite because it forms at high temperatures, where the ferrite field of the phase diagram is known as the delta phase to distinguish it from the low–temperature ferrite phase known as the alpha phase.) The primary factor controlling the ferrite–austenite balance is bulk chemical composition. Chromium, silicon, and molybdenum, and niobium (if present) promote the formation of ferrite, whereas nickel, carbon, manganese, and nitrogen promote the formation of austenite (Peckner and Bernstein, 1977). The nitrogen is introduced during the casting process, but its percentage is not specified. The typical values of nitrogen in the chemical composition of cast stainless steels may vary from 0.03 to 0.08%. Empirical relationships have been developed for estimating the ferrite content from chemical composition; the use of two such relationships are illustrated later in this report (Aubrey et al., 1982; Bonnet et al., 1990).

The size, distribution, and morphology of the ferrite within the austenite depends on solidification conditions during the casting process. The conditions affecting the solidification of metal are complex (Reed–Hill, 1973) and a detailed discussion of them is beyond the scope of this report. Cast stainless steels may solidify with a columnar or equiaxed grain structure or a mixture of both structures. Researchers at Argonne National Laboratory (ANL) have observed that in steels of similar chemical compositions, the average grain size and spacing between ferrite islands generally tends to increase with larger section sizes and corresponding slower heat removal rates.[a] In heavy–wall castings, there can be considerable variations in microstructure across the wall of the casting. The complex nature of metal solidification during casting makes it difficult to predict the finer details of the actual microstructure in the cast stainless steel components of interest in this project. Thus, if knowledge of these microstructural details is important for the assessment of casting integrity and service life, some means of measuring them must be employed.

Increased ferrite content increases the yield and tensile strength of the cast stainless steels, so grades CF–3A and CF–8A have controlled ferrite–austenite ratios to increase the minimum strength levels (Peckner and Bernstein, 1977). The minimum strength levels are indicated in Table 4. These controlled–ferrite grades have the same chemical requirements as CF–3 and CF–8; the ferrite is controlled by adjusting the chemical composition within the limits shown in Table 3. Experience has shown that castings made from the alloys listed in Table 3 may contain up to 30% ferrite when control of the amount of ferrite is not specified.[b] Although ferrite levels near 30% are not usual for castings made in accordance with ASTM specifications (e.g., A–743 and A–744), they are possible.

As shown in Tables 1 and 2, LWR components have been made from CF–8, CF–8A, and CF–8M stainless steel. CF–8 is used for its general resistance to oxidizing conditions. Compared with CF–8, the CF–8M alloy has improved resistance to reducing environments as well as high resistance to oxidizing conditions. Therefore, the CF–8M alloy is widely used for corrosion–resistant pumps and valves. CF–8A is used to provide mechanical strength properties higher than those of the CF–8 alloy. The low–carbon versions (CF–3, CF–3A, and CF–3M) may be used in the future to provide an added margin of resistance to intergranular stress–corrosion cracking (IGSCC), especially in BWRs, where many IGSCC problems in recirculation piping have been encountered in the past (Shah and MacDonald, 1987).

Examples of austenitic–ferritic microstructures observed in cast stainless steel are shown in Figure 4.[c] These samples were obtained from centrifugal castings. The ferrite phase (darkened networks and/or islands) is contained within a matrix of the austenite phase. The sample shown in Figure 4a had about 16% ferrite; the sample shown in Figure 4b had about 28% ferrite. The local chemical composition of the ferrite regions is significantly different from that of the austenite regions in these alloys. To illustrate this point, the local chemical compositions of the samples shown in

a. Private communication with Dr. T. Kassner, Argonne National Laboratory, May 1988.

b. Private communication with D. B. Roach, Battelle Columbus, Ohio, August 22, 1986.

c. C. E. Jaske, unpublished results of studies conducted at Battelle, Columbus, Ohio, 1987.

Table 3. Required chemical compositions of cast stainless steels[a]

Element	Chemical Composition (percent by weight[b])			
	CF–3 CF–3A	CF–8 CF–8A	CF–3M	CF–8M
Carbon	0.03	0.08	0.03	0.08
Managanese	1.50	1.50	1.50	1.50
Silicon	2.00	2.00	1.50	1.50
Sulfur	0.040	0.040	0.040	0.040
Phosphorus	0.040	0.040	0.040	0.040
Chromium	17.0 to 21.0	18.0 to 21.0	17.0 to 21.0	18.0 to 21.0
Nickel	8.0 to 12.0	8.0 to 11.0	8.0 to 12.0	8.0 to 11.0
Molybdenum	0.50	0.50	2.0–3.0	2.0–3.0

a. From Section II – Material Specifications, Part A – Ferrous Materials, 1983 ASME Boiler and Pressure Vessel Code.

b. Maximum except where range is indicated.

Table 4. Required room–temperature tensile properties of cast stainless steels[a]

Property (minimum)	CF–3	CF–3A	CF–8	CF–8A	CF–3M	CF–8M
Tensile strength, MPa (ksi)	485 (70)	530 (77)	485 (70)	530 (77)	485 (70)	485 (70)
0.2% offset yield strength, MPa (ksi)	205 (30)	240 (35)	205 (30)	240 (35)	205 (30)	205 (30)
Elongation in 50 mm or in 2 in.	35.0	35.0	35.0	35.0	30.0	30.0

a. From Section II – Material Specifications, Part A – Ferrous Materials, 1983 ASME Boiler and Pressure Vessel Code.

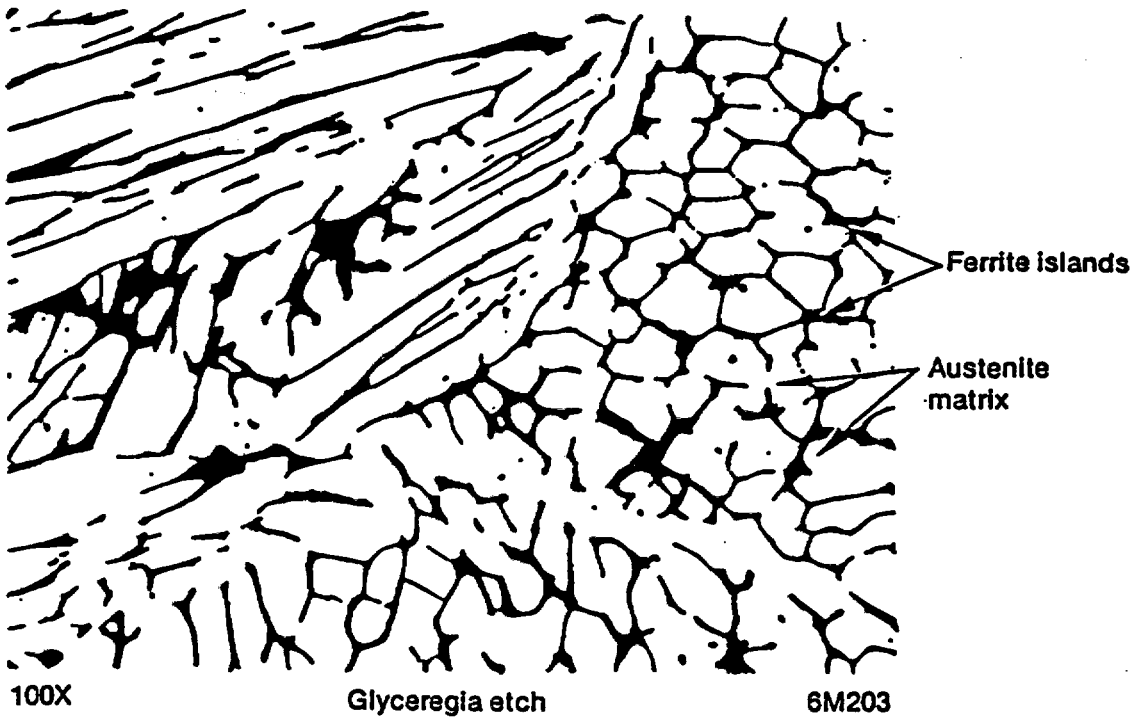

a. CF-8 stainless steel

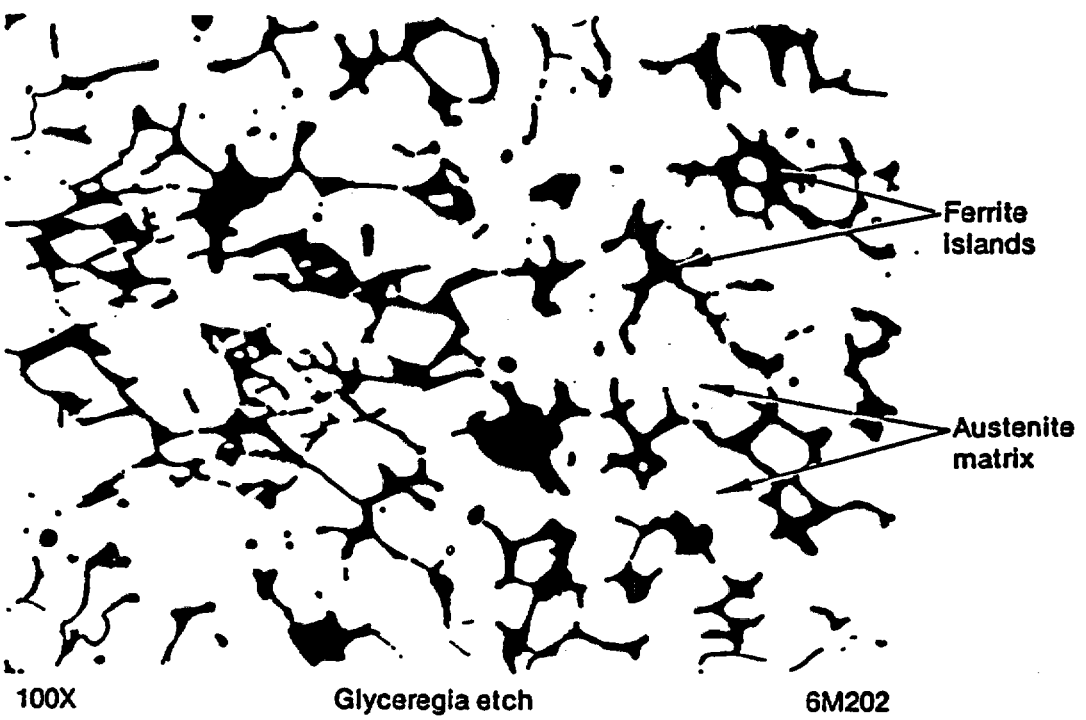

b. CF-8M stainless steel

Figure 4. Typical microstructures of centrifugally cast austenitic–ferritic stainless steels, with islands of ferrite in an austenite matrix.

Figure 4 were analyzed using an electron microprobe; the results are presented in Table 5. The overall bulk composition determined by the foundry is compared with the local composition within the ferrite and the austenite regions. Bulk values for silicon, manganese, sulfur, and phosphorus are not shown in Table 5 because local values were not measured for these four elements. The local values were obtained from the average of six individual determinations at randomly selected regions within each particular phase. As expected, the ferrite phase in both samples contained higher chromium and molybdenum levels and lower nickel levels than the bulk material.

1.3 Benefits of Ferrite in Cast Stainless Steel

Ferrite in cast stainless steel provides resistance to sensitization, which is caused by precipitation of chromium-rich carbides ($M_{23}C_6$) and the resulting depletion of chromium at the grain boundary. Sensitization describes the susceptibility of a stainless steel to intergranular stress-corrosion cracking (IGSCC) following certain heat treatments such as a welding process or a slow cooling from the solution annealing treatment. During welding, temperatures are reached in the heat-affected zone that cause precipitation of chromium carbides. In cast stainless steel, the chromium carbides preferentially precipitate at the ferrite-austenite interfaces, not at the austentite grain boundaries. The faster diffusion rate of chromium in the ferrite phase results in formation of carbides on the ferrite side of the interface. A chromium-depleted zone, which forms on the ferrite side of the interface, is quickly replenished with chromium because of the relatively high chromium content of the ferrite phase (see Table 5) and the high diffusivity of chromium in ferrite. Industrial experience indicates that components with high ferrite levels have more resistance to IGSCC (Peckner and Bernstein, 1977)[a] than do components with low ferrite levels. For example, many duplex (40 to 60%) stainless steels have been found to be highly resistant to IGSCC in aqueous environments in nonnuclear applications (Peckner and Bernstein, 1977).

The minimum amount of ferrite needed to avoid stress-corrosion cracking susceptibility of cast stainless steel in an LWR environment depends on the carbon content in the cast stainless steel; higher carbon

a. Private communication with D. B. Roach, Battelle Columbus, Ohio, August 22, 1986.

Table 5. Results of electron microprobe analysis of two centrifugally cast stainless steel samples

		Chemical Composition[a] (percent by weight)				
Alloy	Region	Fe	Cr	Ni	Mo	C
CF-8	Overall[a]	69.2	20.3	8.40	0.11	0.044
	Austenite	69.6	19.9	8.4	0.03	0.06
	Ferrite	66.7	27.7	3.7	0.06	0.03
CF-8M	Overall[a]	63.7	21.4	9.70	2.81	0.053
	Austenite	63.6	21.3	10.6	2.3	—[b]
	Ferrite	62.0	25.7	6.0	4.0	—[b]

a. Overall composition was determined by ladle analysis as reported by foundry; composition of austenite and ferrite regions was determined by electron microprobe measurements.

b. Value was not determined.

content requires a higher minimum amount of ferrite (Devine, 1980). For example, in a BWR environment cast stainless steel with a maximum carbon content of 0.035% requires a minimum ferrite content of 7.5% for resistance to sensitization during welding (Hazleton, 1988). Results of laboratory tests on CF–3 and CF–8 materials in an accelerated BWR environment show that IGSCC is not expected with a ferrite content greater than 12% (Hughes et al., 1982). In addition, the test results show that no IGSCC effects are expected with a maximum carbon content of 0.03% in weld sensitized material and of 0.015% in furnace–sensitized material, regardless of ferrite content. Similar evaluations for CF–8M material are needed. The test results also show that, in addition to the amount of ferrite, distribution of ferrite or ferrite spacing plays an important role in determining stress–corrosion cracking susceptibility of cast stainless steels. A finer distribution of ferrite provides better resistance to stress–corrosion cracking.

In BWR plants, stress corrosion cracking of the sensitized heat–effected zones of cast stainless steel is possible and has been observed.[a] However, in the worst case, this is likely to result in a local leak rather than in any substantial loss of system integrity, because of the heterogeneous nature of the material. The integrity of weldments is important because welding is used as a joining procedure during fabrication, a method of repairing casting defects during fabrication, an installation procedure, and a method of repairing components for the purpose of extending their operational lifetimes.

The presence of some ferrite (typically at least 5%) minimizes the occurrence of hot cracking or microfissuring in castings and weld metal.[b] In several older plants, the weld metal in the pump casing and in stainless steel RCS piping have less than 3% ferrite, whereas in newer plants a minimum of 5% ferrite is required for the reactor coolant pressure boundary components (USNRC, 1978).

a. Private communication with M. E. Lapides, Electric Power Research Institute, Palo Alto, California, 1990.

b. Private communication with E. Landerman, consultant, Pittsburgh, Pennsylvania, September 1988.

2. REVIEW OF INFORMATION ON THERMAL EMBRITTLEMENT

Understanding the basic mechanisms that cause thermal embrittlement damage to stainless steel components is necessary for identifying the aging parameters related to design, fabrication, and operation of these components. The degree of material embrittlement in aged cast stainless steel components is most often evaluated by Charpy V-notch (CVN) impact energy tests and, recently, by fracture toughness tests. Tensile and fatigue properties for the aged components also are needed in evaluations of the integrity of the cast stainless steel components. This section reviews the basic mechanisms causing thermal embrittlement damage, evaluates the currently available Charpy impact energy and fracture toughness data, and then briefly discusses the low-cycle fatigue behavior of the cast stainless components.

2.1 Basic Mechanisms

The mechanisms of thermal aging that cause embrittlement in cast stainless steels have been reviewed and evaluated extensively by Chopra and Chung (1985, 1986a, 1986b, 1986c, 1987, 1990a, 1990b), Chung and Chopra (1987), Chung (1989), Chopra and Sather (1990), Chopra (1990), Auger et al. (1990), Bonnet et al. (1990), and Brown et al. (1990). Embrittlement or loss of toughness in cast stainless steels during elevated-temperature exposure is related (a) to the precipitation of carbides at the austenite–ferrite phase boundaries and (b) to the formation of the Cr-rich alpha-prime phase and the Ni-rich and Si-rich G phase in the ferrite. The phase-boundary carbides play a significant role in embrittlement for exposures at temperatures greater than 400°C (750°F), but have less effect on the embrittlement at exposure temperatures less than 400°C.

For LWR operating temperatures [less than 350°C (660°F)], the formation of the alpha-prime phase and the G phase in the ferrite are the primary factors involved in embrittlement. Also, the kinetics of the formation of these phases appear to be different at temperatures less than 400°C (750°F) than at temperatures greater than 400°C. Because of these differences in formation and precipitation behavior, the results of tests on material subjected to accelerated aging at temperatures greater than 400°C should not be extrapolated to the lower LWR operating temperatures. Bamford et al. (1987) of Westinghouse describe the results of analyses performed using x-ray energy dispersive spectroscopy. These results indicate that data from accelerated aging studies at temperatures greater than 400°C (750°F) could be used to predict behavior at operating temperatures. Additional, independent research is needed to resolve the differences between the ANL and Westinghouse studies.

The alpha-prime phase typically forms by the process of spinodal decomposition (Chopra and Chung, 1987, Sassen et al., 1987). Spinodal decomposition refers to the reaction whereby two phases of the same crystal lattice type, but different compositions and properties, form because a miscibility gap exists in the alloy system. In the iron–chromium system, these immiscible phases are known as the iron-rich alpha phase and the chromium-rich alpha-prime phase. This phase separation process occurs at a very fine scale (on the order of only a few nanometers) in the ferrite regions of cast stainless steel, and use of the atom probe field ion microscope is required to resolve the presence of the alpha-prime phase (Sassen et al., 1987). There are indications that after extensive (many years) aging at LWR operating temperatures the alpha-prime phase can form also by means of a nucleation and growth process, as well as by spinodal decomposition (Chopra and Chung, 1987). Depending on the composition of the ferrite and the exposure temperature, either or both of these processes may be involved in the formation of alpha-prime phase.

The G phase forms in the ferrite by a nucleation and growth process, and its rate of formation increases with increased levels of carbon and molybdenum (Chopra and Chung, 1987). But the G phase has no direct effect on the degree of embrittlement, as demonstrated by the following laboratory test. A CF-8 stainless steel pump cover was found to be embrittled after 12 years of service in a BWR (Chopra and Chung, 1987). Annealing for one hour at 550°C (1020°F) dissolved the alpha-prime phase and restored the Charpy-impact resistance to the level expected for unaged material, but had no effect on the G phase present. Thus, the G phase had no significant effect on the degree of embrittlement, and the alpha-prime embrittlement was easily reversed by a short heat treatment (one hour) at a moderate temperature [550°C (1020°F)].

The annealing treatment described above was applied to verify that embrittlement was caused by the alpha prime. It is not proposed as a method for reversing the effects of alpha-prime embrittlement in actual components because of the practical difficulties that

would be encountered in applying such a heat treatment in the field.

The presence of G phase may indirectly affect the degree of embrittlement in cast stainless steel components; however, its role is not yet well-defined. Its presence apparently mitigates the degree of embrittlement caused by the alpha-prime phase by slowing down its formation. On the other hand, the G phase (and perhaps the alpha-prime phase) precipitates more readily at dislocations (Chopra and Chung, 1987). Thus, cold work or stressing during service, including fatigue cycling, may increase the degree of embrittlement; no data on this potential effect were found in the present project.

Because only the ferrite phase is embrittled by long-term service at LWR operating temperatures, the overall thermal embrittlement of a cast stainless steel product depends on the amount and morphology of the ferrite present. For LWR applications, a current guideline is that low-temperature embrittlement is a major concern only when the volume fraction of ferrite exceeds a level of approximately 15% (Copeland and Giannuzzi, 1984). The reasoning behind this guideline is that the ferrite phase tends to form in isolated pools contained within the austenite when ferrite levels are less than or equal to 15%. In this case, the overall toughness of the stainless steel casting is not greatly affected even if the ferrite were embrittled. However, where ferrite levels are greater than 15%, there is a greater tendency for a continuous path of embrittled material to exist through the thickness of the cast component, which would greatly reduce its toughness if the ferrite regions were embrittled (Chopra and Chung, 1986b).

There is recent evidence that thick-walled (typically greater than 100 mm) stainless steel castings with ferrite levels in the range of 10 to 15% also may be subject to low-temperature embrittlement (Chopra and Chung, 1986b). In heavy-section castings, the grain size tends to be large and the ferrite spacing (average distance between ferrite islands) is increased. With increasing ferrite spacing at a constant ferrite content, the tendency for a continuous path of ferrite to exist through the thickness of the cast component increases. Bonnet et al. (1990) selectively dissolved the austentite phase from samples of CF-8M and found that the ferrite phase remained continuous at ferrite volume fractions as low as 5%. This result indicates that a relatively small amount of ferrite may provide a continuous path for fracture in aged cast stainless steels.

Two different sets of data have recently been presented regarding the thermal embrittlement of stainless steel weldments. One data set indicates that the fracture toughness of Type 308 SS weldments was not affected by aging at 427°C (800°F) for 10,000 h (Mills, 1987). However, the other data set indicates that the Charpy V-notch impact energy of Type 308 SS weldments with 8% ferrite may be significantly reduced by aging at 343°C for 10,000 h; however, corresponding fracture toughness data are not presented. More research is needed to ensure that the fracture toughness of the weldments for cast stainless steel components is not significantly affected by thermal aging at the LWR operating temperatures.

Embrittlement of welds, if confirmed by test results, could become a major problem because welds generally have lower initial fracture toughness before thermal exposure than base metal. Weldments in stainless steel castings may contain high residual stresses that approach the yield strength (Egan et al., 1987) because Section III of the ASME Boiler and Pressure Vessel Code neither requires nor prohibits postweld heat treatment of these welds. The usual industry practice is to not subject welds in cast stainless steel components to postweld heat treatments, because such a heat treatment might sensitize base material near the end of the heat-affected zone and make that region susceptible to IGSCC.

2.2 Charpy Impact Energy Data

The degree of low-temperature embrittlement is most often quantified by the room-temperature Charpy impact energy after aging at temperatures in the range of 300 to 450°C (570 to 840°F). Increased aging temperature is employed to accelerate the rate of thermal embrittlement compared with that which occurs at normal LWR operating temperatures near 288°C (550°F). Charpy V-notch impact energy data, obtained from Chopra (1990), for thermally aged CF-3, CF-8 and CF-8M stainless steel are shown in Figures 5, 6, and 7, respectively. In each figure, the Charpy impact energy is plotted as a function of the aging parameter P, which is defined by the following relation:

$$P = \log_{10} \{t/\exp[(Q/R)(1/T - 1/673)]\} \qquad (1)$$

where t is the time, Q is the activation energy, R is the gas constant, and T is the absolute temperature. P is defined such that it is equivalent to the logarithm (base 10) of the number of hours of aging at 400°C (750°F). For example, a value of P = 4 is equivalent to aging for 10,000 h at 400°C.

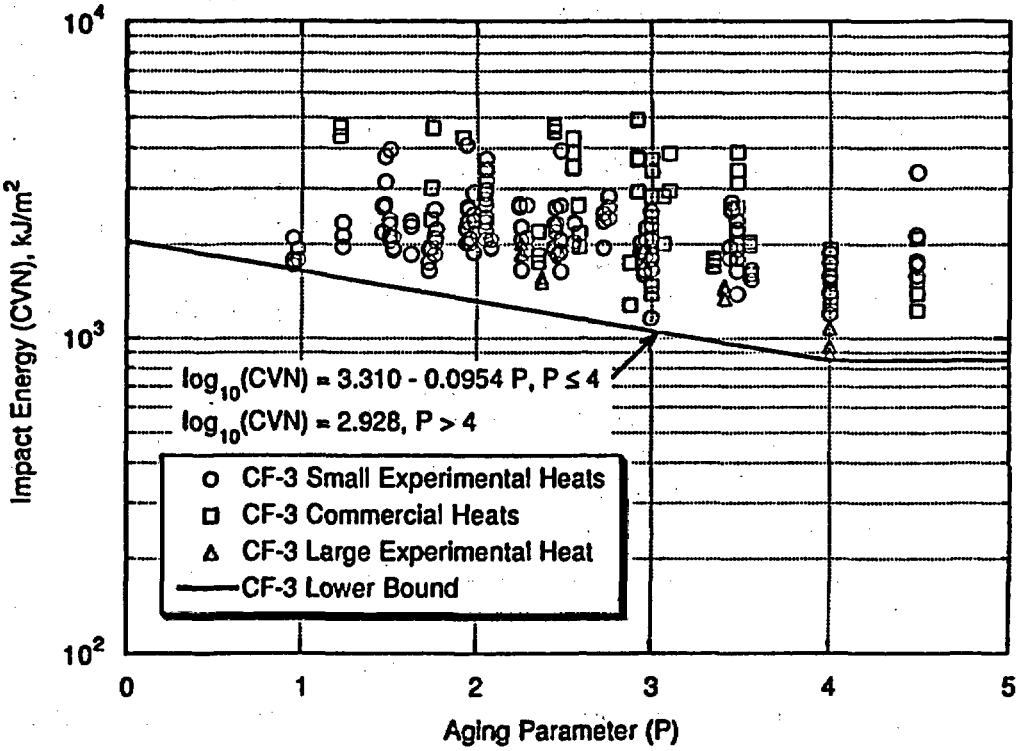

Figure 5. Effect of thermal aging on the room-temperature Charpy V-notch impact energy of CF-3 stainless steel.

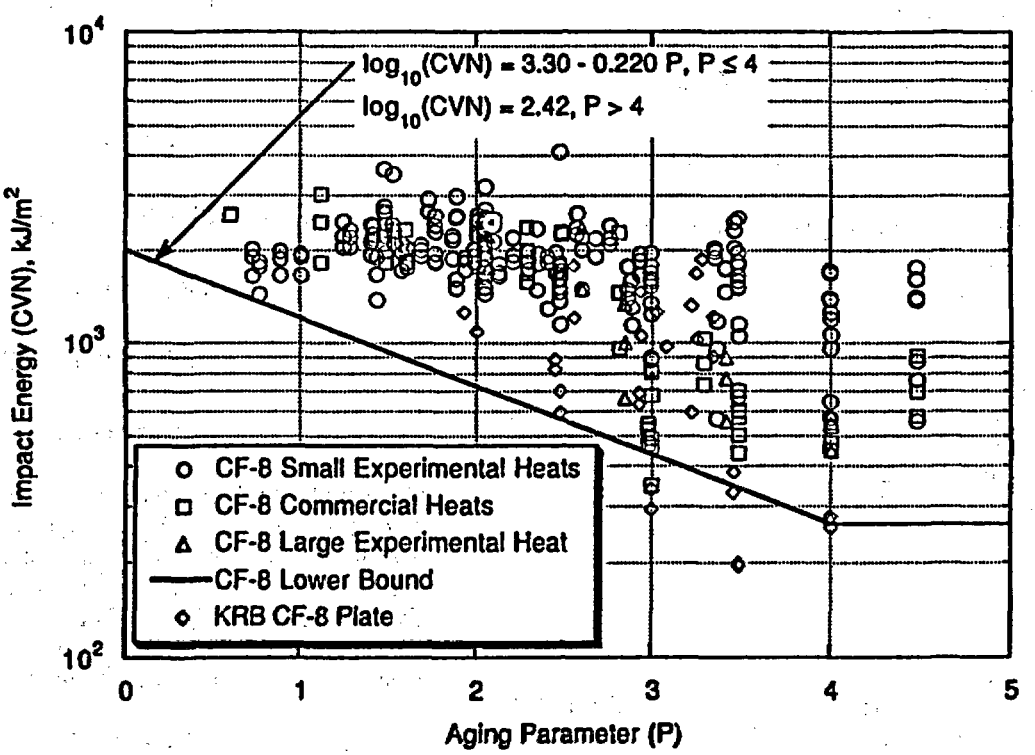

Figure 6. Effect of thermal aging on the room-temperature Charpy V-notch impact energy of CF-8 stainless steel.

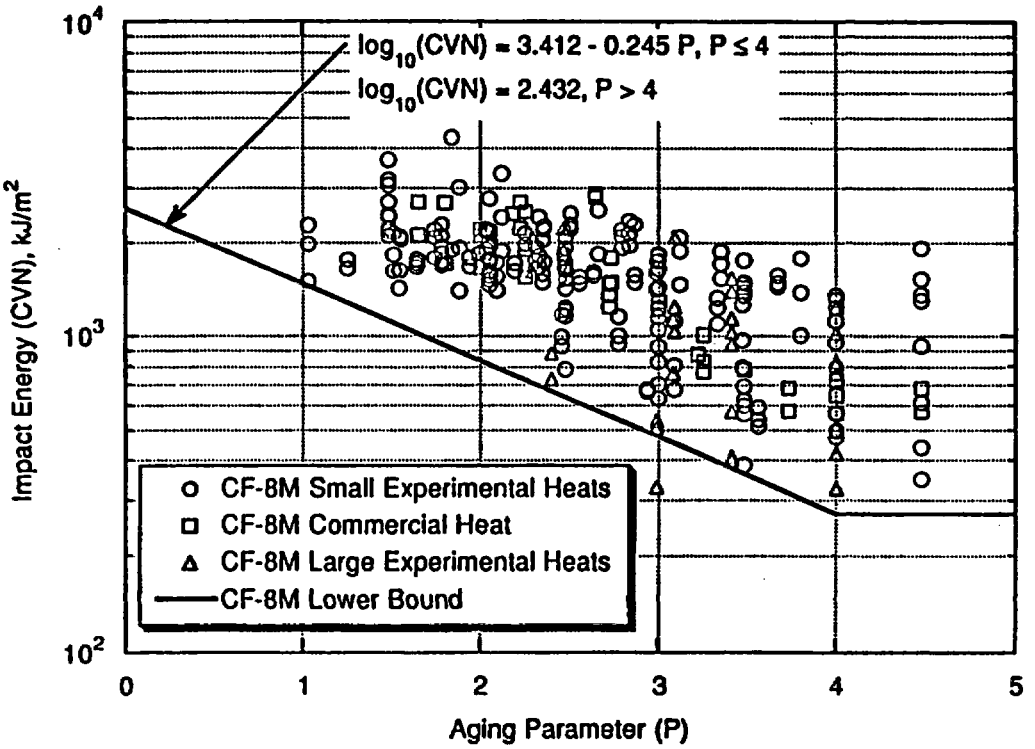

Figure 7. Effect of thermal aging on the room–temperature Charpy V–notch impact energy of CF–8M stainless steel.

From multiple correlation analysis of data on the aging of cast stainless steels, the activation energy was found to be related to composition by the following approximate relation:[a]

$$Q\ (kJ/mole) = -182.6 + 19.9(\%Si) + 11.08(\%Cr) + 14.4(\%Mo) \quad (2)$$

where the percentages are in terms of weight. Equations (1) and (2) were used by Chopra and Chung in their earlier work.

Recently, Chopra and Chung (1989a and 1989b) have developed new correlations for predicting the activation energy. They found the following separate correlations for the Swiss data (Trautwein and Gysel, 1982) and the Framatome[a]–ANL (Chopra and Chung, 1989a and 1989b) data, respectively:

$$Q(kJ/mole) = -66.70 + 6.91(\%Cr) - 5.44(\%Ni) + 8.08(\%Mo) + 17.2(\%Si) + 44.1(\%Mn) + 297(\%N)$$

(Swiss data) (3)

$$Q(kJ/mole) = 90.60 + 9.63(\%Cr) - 8.12(\%Ni) - 7.54(\%Mo) + 20.6(\%Si) - 123(\%Mn) + 318(\%N)$$

(Framatome – ANL data) (4)

Compared with Equation (2), Equations (3) and (4) include additional terms for nickel, manganese, and nitrogen as well as those for chromium, molybdenum, and silicon. The contribution of molybdenum is positive in Equations (2) and (3) but negative in Equation (4). Also, the contribution of manganese is positive in Equation (3) but negative in Equation (4).

Chopra and Chung (1989a and 1989b) argue that Equation (4) is the most appropriate to use in assessing

a. Unpublished paper presented by G. Slama et al., at SMiRT Postconference Seminar 6 at Monterey, California, August 29–30, 1983.

the potential for thermal embrittlement of cast stainless steel components that are used in U.S. nuclear plants because the compositions included in the Framatome–ANL set of data are more representative of those used in such components. For this reason, Equation (4) was used, along with Equation (1), in computing the values of P plotted in Figures 5 through 7. The values of Q and P were calculated from the data supplied by Chopra and Sather (1990). Although Equation (4) provides an improvement over Equation (2), there is still room for improvement in this analytical approach, as is evidenced by the wide scatter of the data in Figures 5 through 7. Furthermore, Chopra and Sather (1990) reported that the correlation represented by Equation (4) was developed for observed values of Q between 75 and 240 kJ/mole. Thus, it should be used only for cases where the computed value of Q falls within this range.

The compositions included in the Swiss set of data fall in a relatively narrow range that does not represent those used in cast stainless steel castings produced in the U.S. Equation (1) and either Equation (2), (3), or (4) should be used to estimate the degree of aging of a specific heat of material during service. However, because the reasons for the differences among Equations (2), (3), and (4) are not completely understood, additional research concerning the factors contributing to the activation energy for thermal aging of cast stainless steels is needed.

The recent work by Bonnet et al. (1990) even questions the validity of using an empirical value of Q calculated from the chemical composition. They believe that Q is a function of the aging temperature and approaches a value of approximately 250 kJ/mole at 300 to 325°C, the region of primary interest for LWR applications. If this belief is true, it implies that values of Q calculated using Equation (4) provide overly pessimistic predictions of the aging kinetics for cast stainless steels. Unfortunately, their conclusion is based on the evaluation of data for only two heats of CF–8M stainless steel. Additional, extensive evaluations would be required before their approach could be applied to the assessment of aging in LWR cast stainless steel components.

Figures 5 through 7 show lower–bound approximations to the data trends for each alloy. These approximations were developed as part of the work in the current project. The impact energy decreases as a function of P for values of P less than about 3.5 to 4. For values of P greater than about 3.5 to 4, the impact energy appears to show no further decrease as a function of P. In fact, it even shows a slight increase. Thus, the effect of aging on Charpy–impact energy appears to saturate at long times. As a conservative approximation, the lower–bound CVN–vs.–P lines were assumed to saturate at the CVN value where P was equal to 4 (as shown in Figures 5 through 7).

All of the CVN data for CF–3M fell above the lower–bound approximation, as is shown in Figure 5. Some of the data for the KRB plate[a] fell below the lower–bound approximation for CF–8 (see diamond symbols in Figure 6); these data were discounted in developing the lower–bound approximation because they are from European material rather than from U.S. material. One of the data points for the commercial heats (see square symbol in Figure 6) fell slightly below the lower–bound approximation because it was considered to be an outlier. Also, for the same reason, one of the data points for the large experimental heats (see triangular symbols in Figure 7) fell below the lower–bound approximation for CF–8M. The lower–bound approximations for CF–8 and CF–8M were almost the same, whereas that for CF–3 was higher than the other two. This result, as is discussed later in this report, implies that the maximum degree of thermal embrittlement is controlled by factors other than just the chemical composition.

These lower bounds are appropriate for LWR applications because operating temperatures less than 400°C are expected and the degree of embrittlement at these lower temperatures is not expected to exceed that observed at 400°C. It would be useful, in future work, to verify this assumption by evaluating the impact behavior of materials that have been exposed to temperatures of 300°C (570°F) or less for many years. Because a greater degree of embrittlement is expected from exposures at 400°C (750°F) than from exposures at 350°C or less, using lower bounds to all of the data should provide conservative, but overly pessimistic, predictions of thermal embrittlement. Additional thermal embrittlement data for the values of aging parameter P greater than 4 are needed to verify that the lower bound curve levels off, especially at temperatures of 350°C or less.

The failure of P to fully correlate the changes in impact energy as a function of aging time and temperature indicates that the simple expression of Equation (4) does not accurately model the activation energy for the complex process of thermal embrittlement, which involves the formation of carbide, alpha–prime, and G–phase precipitates and their interactions during aging at temperatures in the range of 300 to 450°C (570 to 840°F) (Chopra and Chung, 1986c).

a. From KRB reactor at Gundremmingen, West Germany.

However, until a more accurate model can be developed, the lower bounds shown in Figures 5 through 7 provide guidance for LWR applications and indicate an approach that should be developed further.

Most of the data that have been developed to assess the effects of thermal embrittlement of cast stainless steels are room–temperature impact properties, such as those shown in Figures 5 through 7. For application to LWR components, properties at operating temperature are needed. Also, fracture toughness and tearing modulus data, rather than impact energy data, are needed in fracture–mechanics assessments of the safety of components. Both of these issues are being addressed in recent work (Landerman and Bamford, 1978; Buchalet et al., 1985; Chopra and Chung, 1989b; Hiser, 1987; Bamford et al., 1987).

Figures 8, 9, and 10 show Charpy V–notch impact data for CF–3, CF–8, and CF–8M, respectively, as a function of test temperature. Except for Figure 8c, the open circles represent data for unaged material, the filled triangles represent data for material aged approximately 10,000 hours at 350°C, and the filled squares represent data for material aged approximately 10,000 hours at 400°C. In Figure 8c, the circles represent data for unaged material, the triangles represent data for material aged 9,980 hours at 350°C, and the squares represent data for material aged 30,000 hours at 350°C (Figure 8c contains no data for material aged at 400°C). The filled symbols in Figure 8c are for specimens with a L–C orientation (longitudinal specimen with circumferential crack), and the open symbols in Figure 8c are for specimens with a C–L orientation (circumferential specimen with longitudinal crack).

Aging typically reduced the impact resistance of the materials at all test temperatures, except for the centrifugally cast pipe (see Figure 8c), where the aged material had the same upper–shelf impact resistance as the unaged material. The centrifugally cast pipe also had significantly higher impact resistance than the statically cast materials, and within the normal scatter of the data, the specimen orientation (L–C versus C–L) had no significant effect on its impact resistance. The impact resistance of the materials aged at 400°C was always slightly less than that of the materials aged at 350°C. For the aged materials, the room–temperature (25°C) data always provided a conservative estimate of the impact resistance at typical LWR operating temperatures (up to approximately 290°C). Thus, when no high–temperature Charpy data are available, the lower bound to the room–temperature Charpy data is likely to provide a conservative estimate of the lower bound to the high–temperature Charpy data.

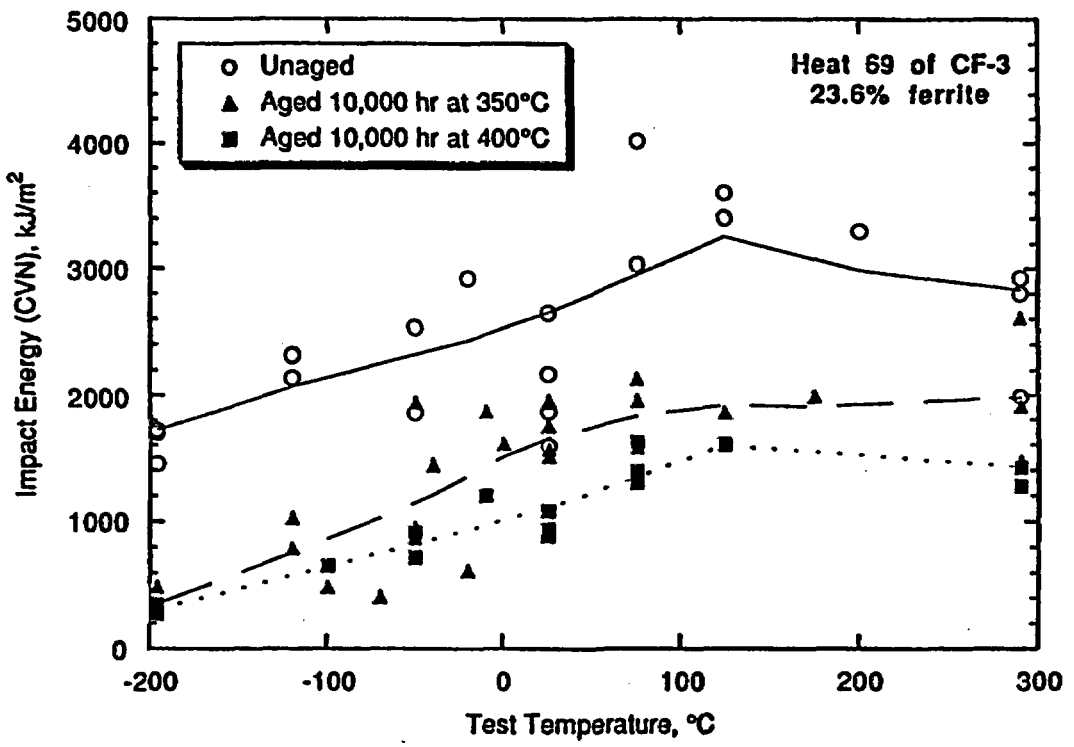

a. Cast 76–mm slab, Heat 69.

Figure 8. Effect of test temperature and thermal aging on the Charpy V–notch impact energy of CF–3 stainless steel, data from Chopra and Sather (1990).

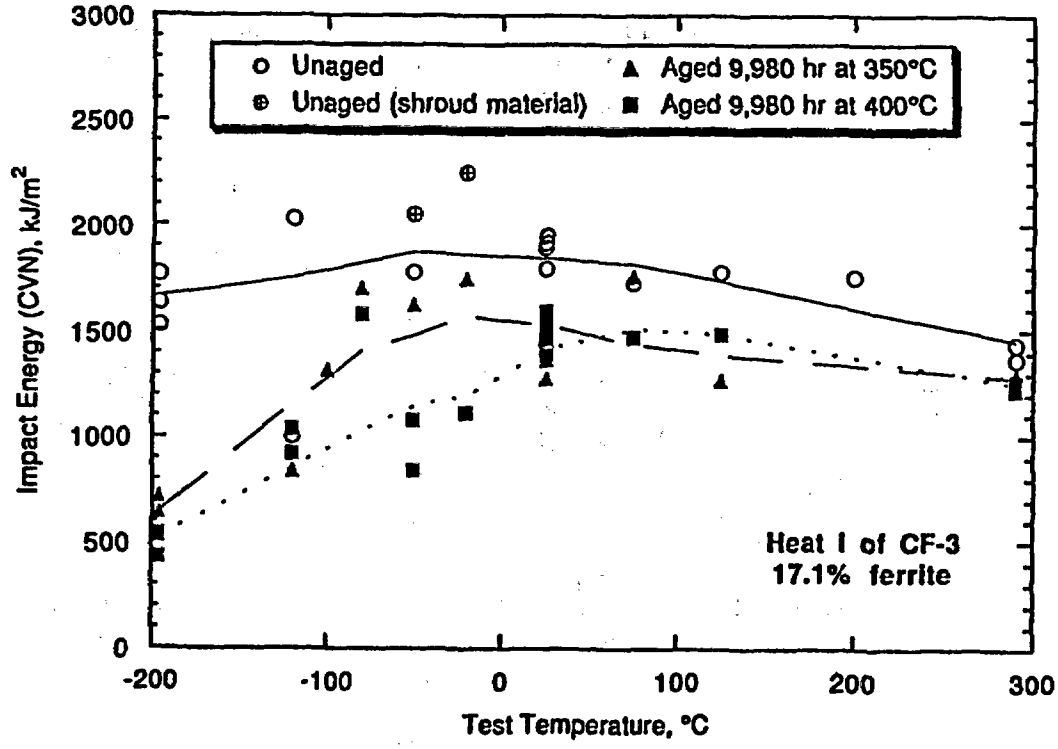

b. Cast pump impeller vanes, Heat 1.

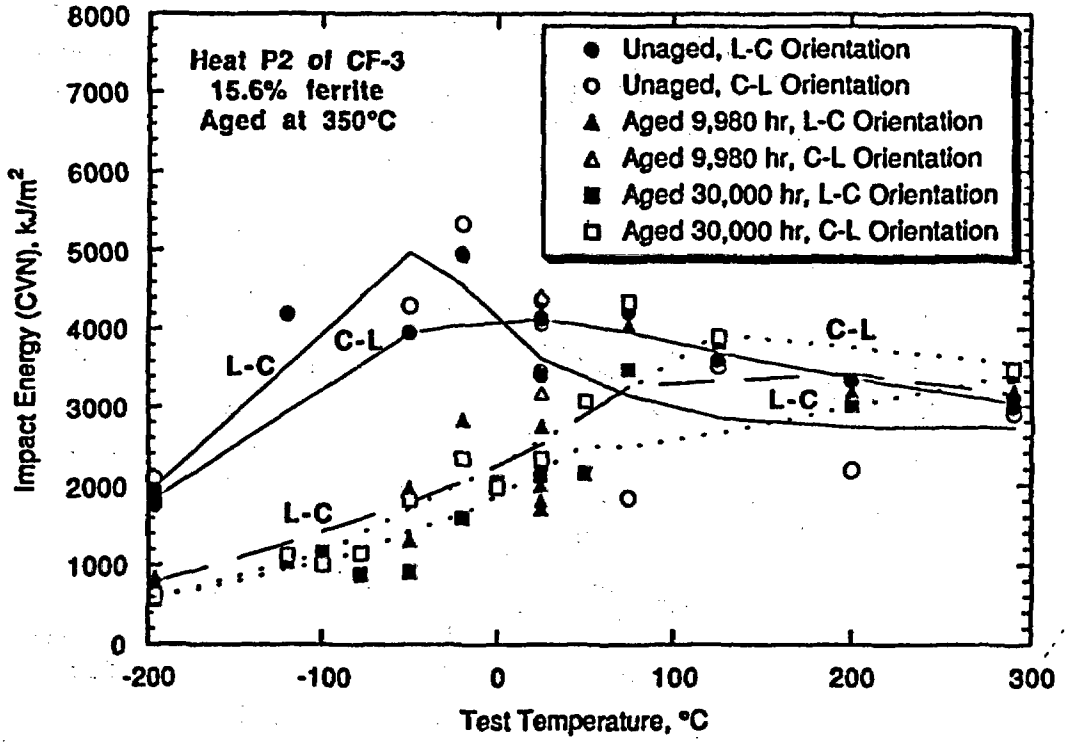

c. Centrifugally cast pipe, Heat P2.

Figure 8. Effect of test temperature and thermal aging on the Charpy V-notch impact energy of CF-3 stainless steel, data from Chopra and Sather (1990). (Continued.)

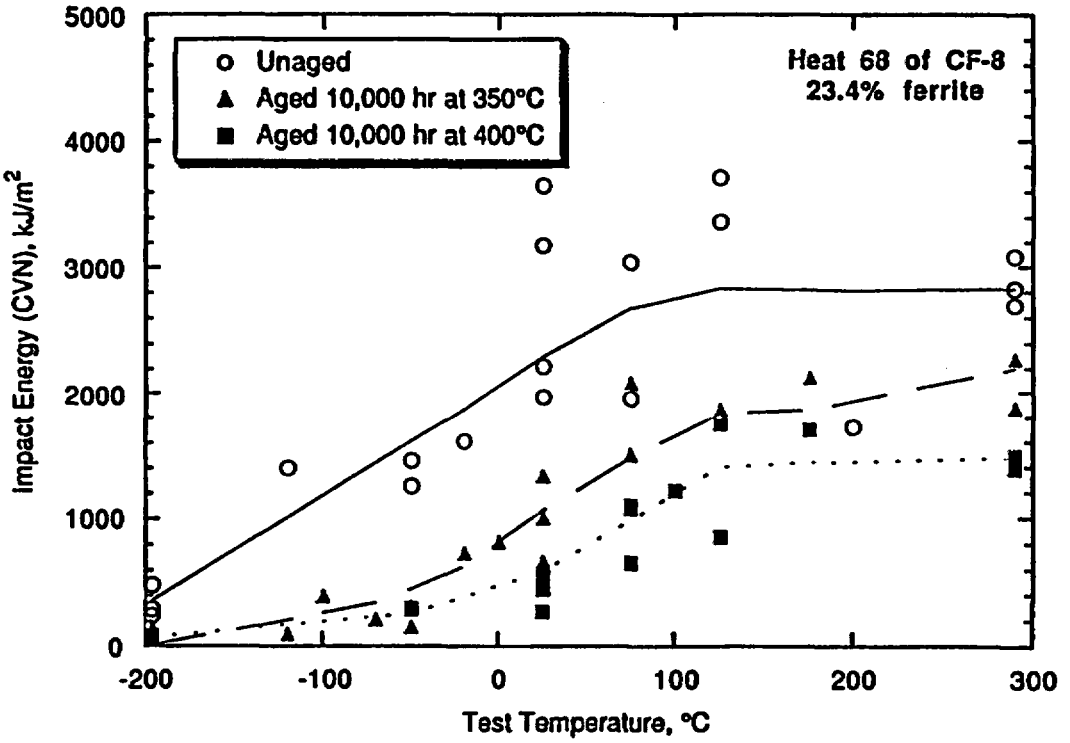

Cast 76-mm slab.

Figure 9. Effect of test temperature and thermal aging on the Charpy V-notch impact energy of CF-8 stainless steel, Heat 68 data from Chopra (1990).

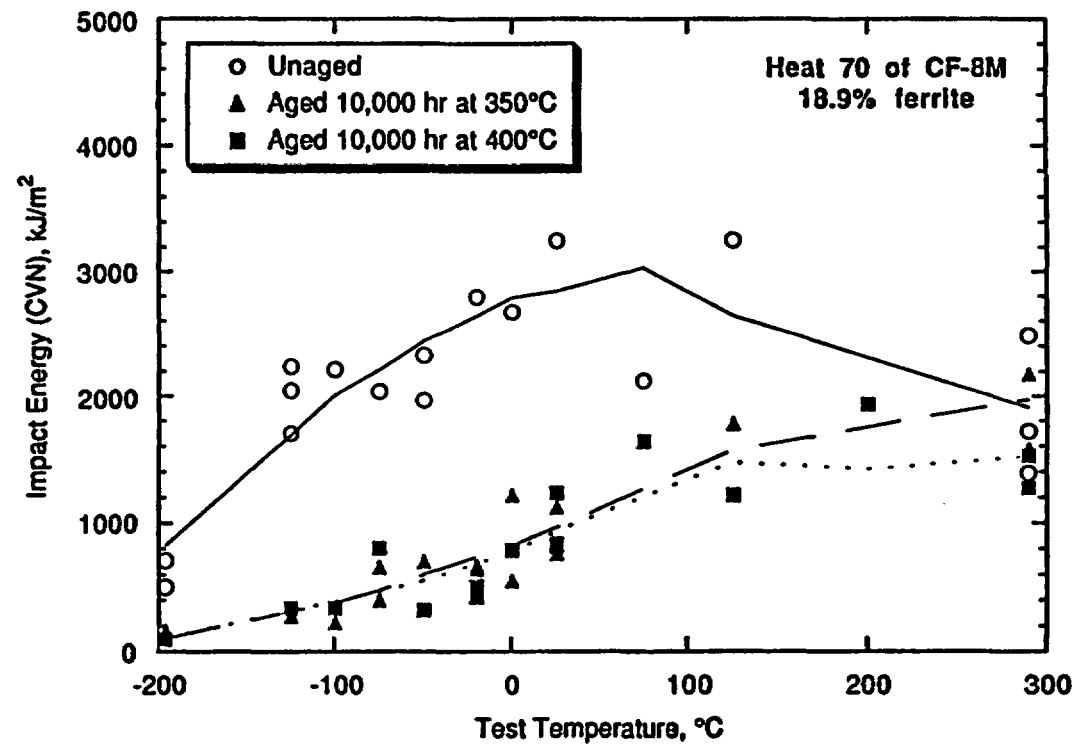

a. Cast 76-mm slab, Heat 70.

Figure 10. Effect of test temperature and thermal aging on the Charpy V-notch impact energy of CF-8M stainless steel data from Chopra and Sather (1990).

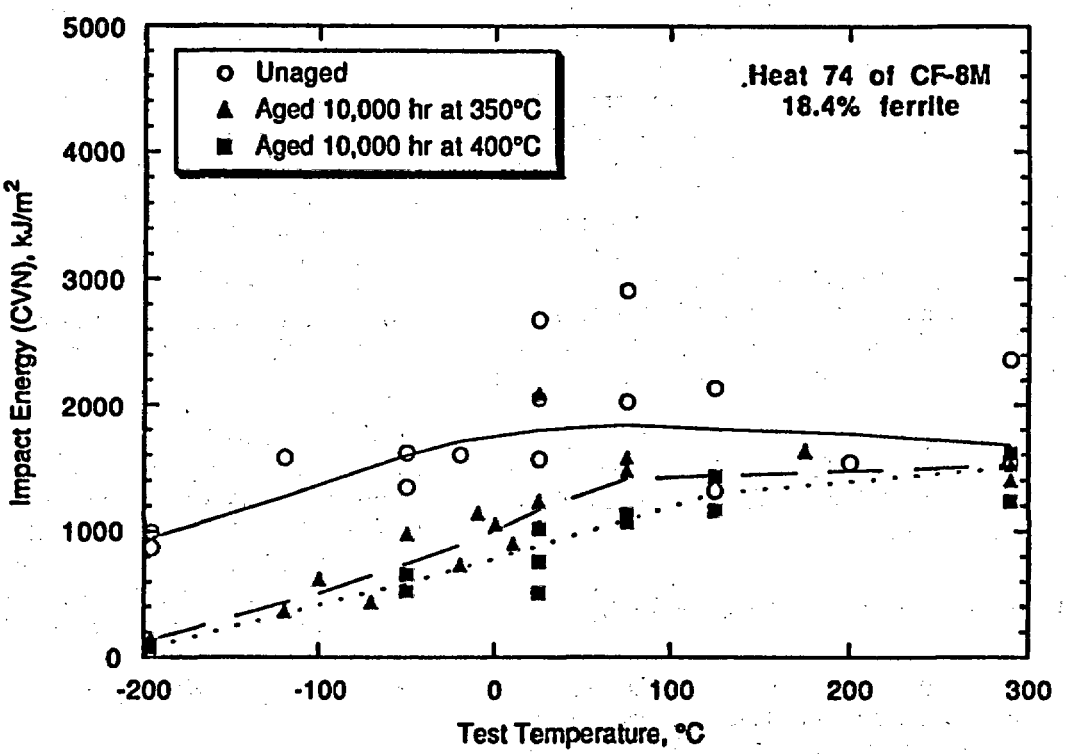

b. Cast 76–mm slab, Heat 74.

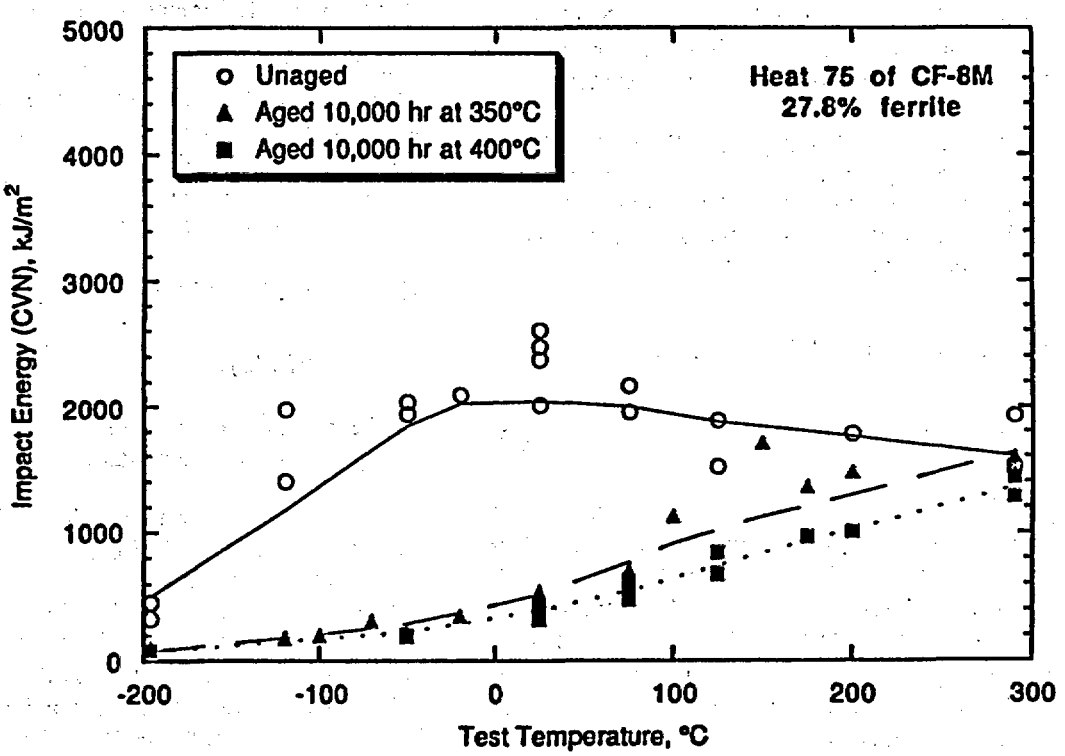

c. Cast 76–mm slab, Heat 75.

Figure 10. Effect of test temperature and thermal aging on the Charpy V–notch impact energy of CF–8M stainless steel data from Chopra and Sather (1990). (Continued.)

The curves shown in Figures 8 through 10 are best fits to the data obtained by means of locally weighted least-squares regression, using weighting factors (degree of data smoothing) of 66 to 75 percent. There are no explicit expressions for these curves; they were obtained to graphically show the trends of the data rather than to provide mathematical expressions for computing CVN values. In general, the transition region of these curves shifted to higher temperatures and the upper-shelf energy (USE) decreased with increased aging temperature or time. In many cases, the USE reached a peak at some temperature less than 300°C and decreased at temperatures above that peak.

In contrast to the preceding curve fitting approach, Chopra and Chung (1990a) used a hyperbolic tangent function of the following form to describe Charpy transition curves:

$$CVN = K_o + B\{1 + \tanh[(T-C)/D]\}$$

where K_o is the lower-shelf energy, T is the test temperature, B is the half-distance between the upper- and lower-shelf energy, C is the mid-shelf transition temperature in °C, and D is the half-width of the transition region. This approach has the advantage of providing an explicit description of the Charpy transition curves, but it does not completely model the observed trends of the experimental result. For this reason, the approach was not employed in the current study.

In their recent work, Chopra and Chung (1989a and 1989b) have proposed the following parameter for correlating the minimum Charpy V-notch impact energy after long-term aging with the composition and microstructure of cast stainless steels:

$$\Phi = \delta_m^2 \, [\%C + 0.4(\%N)] \, (\%CR + \%Mo + \%Si) \, L \, (10^{-3}) \qquad (5)$$

where δ_m is the measured volume fraction of ferrite in percent and L is the mean ferrite spacing in μm. Their correlation between the parameter Φ and the minimum room-temperature Charpy V-notch impact energy is shown in Figure 11. The power-law equation shown in Figure 11, $CVN = 6{,}270 \; \Phi^{-0.6112}$, was obtained by least-squares regression analysis of the data in that figure as part of the work in the current study. Except for the Framatome data point (filled triangle), the correlation appears to be reasonable. Additional work should be performed to evaluate the correlation of this parameter with the minimum high-temperature Charpy V-notch impact energy data and with fracture-toughness data at both room and elevated temperatures. The Φ parameter could be used, with either (a) measured values of the ferrite fraction and spacing or (b) a calculated value of the ferrite fraction and an estimated upper-bound (worst-case) value of the ferrite spacing, to estimate the minimum room-temperature Charpy impact energy expected after long-term aging of a cast stainless steel. In either case, it would be necessary to know the composition of the stainless steel, including the nitrogen content.

Chopra and Chung (1990a) have recommended that a worst-case value for the ferrite spacing of 180 μm be used when a measured value is not available. For example, for a CF-8 stainless steel with 0.05%C, 0.07%N, 20.6%Cr, 8.3%Ni, 0.3%Mo, 1.1%Si, and a measured ferrite content of 15%, the value of Φ is computed to be 69.5 for a ferrite spacing of 180 μm. Then, the equation shown in Figure 11 gives

$$CVN = 6{,}270 \; \Phi^{-0.6112} = 6{,}270 \; (69.5)^{-0.6112}$$

$$= 469 \text{ kJ/m}^2$$

for the minimum room-temperature Charpy-impact energy expected after long-term aging.

If it were decided that the CVN value based on the worst-case ferrite spacing were lower than desired, the actual ferrite spacing could be measured and used in the correlation. For example, if the ferrite spacing for this CF-8 stainless steel were measured to be 100 μm, the value of Φ would be 38.6, giving

$$CVN = 6{,}270 \; \Phi^{-0.6112} = 6{,}270 \; (38.6)^{-0.6112}$$

$$= 672 \text{ kJ/m}^2$$

for the minimum room-temperature Charpy-impact energy expected after long-term aging.

This Φ-parameter approach provides a simple, straightforward method of estimating the minimum room-temperature Charpy-impact energy expected for a cast stainless steel after long-term service. Chopra and Chung (1990a) also have shown that the Φ parameter can be used to provide improved correlations for aging kinetics. They found improved correlations between impact energy and the aging parameter P when the materials were grouped by the value of Φ rather than by alloy type, as in Figures 5, 6, and 7. This approach should be evaluated further.

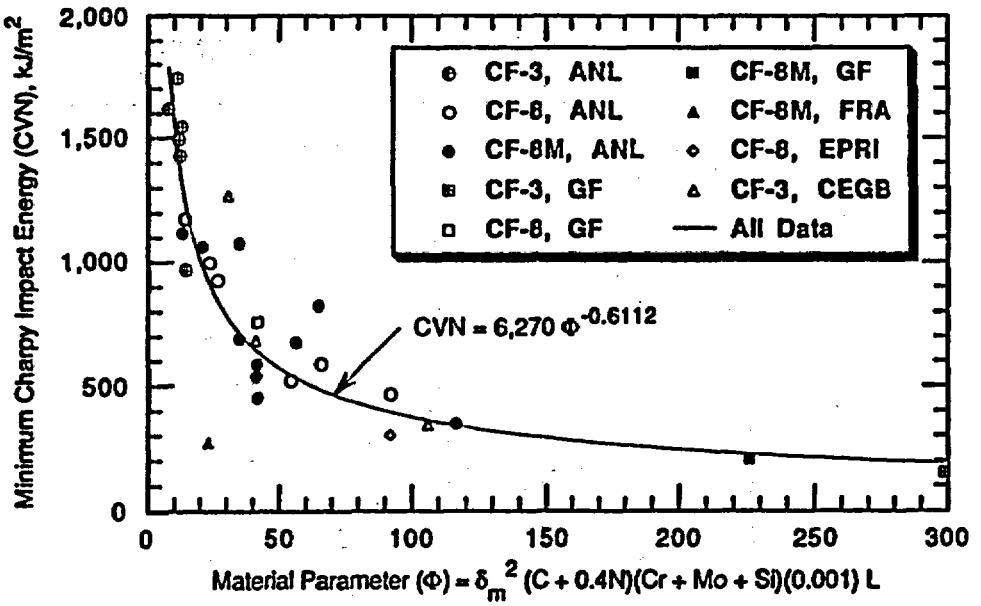

Figure 11. Correlation between minimum room-temperature Charpy V-notch impact energy and material parameter Φ for aged cast stainless steels, adapted from Chopra and Chung (1989b), data supplied by Chopra in June 1990.

2.3 Fracture Toughness Data

The fracture toughness of cast stainless steels has been evaluated by means of J-R curve tests (Bamford et al., 1985; Chopra and Chung, 1987; Hiser, 1987).[a] Most of the earlier testing (Bamford et al., 1985)[a] was performed at room temperature, but some of the recent testing (Chopra and Chung, 1987; Hiser, 1987) has been performed at 290°C (555°F). Those investigations included analyses of test results to determine values of J_{Ic}, which is a measure of fracture toughness at the initiation of crack growth in metallic materials, and tearing modulus, T, which is proportional to the derivative of fracture tougness J with respect to crack size, as covered by the test procedures described in ASTM Designation E 813.

Figures 12 through 15 show fracture-toughness data correlations for cast stainless steels, as taken from the work of Chopra and Chung (1990a). The data shown in these figures are from Argonne National Laboratory (ANL) (Chopra and Chung, 1989a and 1989b), Westinghouse (WH) (Landerman and Bamford, 1978; Bamford et al., 1985), Framatome[a] (FRA), Electric Power Research Institute (EPRI), Battelle (BAT), and KRB. Figure 12 shows the correlation between room-temperature fracture toughness, J_{Ic} and room-temperature impact energy. The solid curve represents the mean trend of the data, whereas the chain-dashed line represents the lower bound to the data. In performing a structural integrity evaluation, the lower-bound relationship can be used to estimate the room-temperature fracture toughness from an estimated or measured value of the room-temperature impact energy for a specific component. Then, the estimated room-temperature fracture toughness can be used to estimate a lower-bound value of the room-temperature tearing modulus using the dashed line in Figure 13. As is shown in Figure 14, the lower-bound fracture toughness at room-temperature correlation from Figure 12 also provides a conservative estimate of the fracture toughness at 290°C from a value of room-temperature Charpy impact energy. Finally, the tearing modulus at 290°C can be estimated from the lower-bound correlation (dashed line) shown in Figure 15. If fracture toughness could be obtained for aged material from the component being evaluated in a structural integrity assessment, it could be used in place of values estimated using the preceding scheme.

The value of fracture toughness at a temperature between the room temperature and 290°C can be estimated by linearly interpolating between the data presented in Figures 12 and 14; similarly, the value of tearing modulus can be obtained from the data presented in Figures 13 and 15. The values of fracture

a. Unpublished paper presented by G. Slama et al. at SMiRT Postconference Seminar 6 at Monterey, California, August 29–30, 1983.

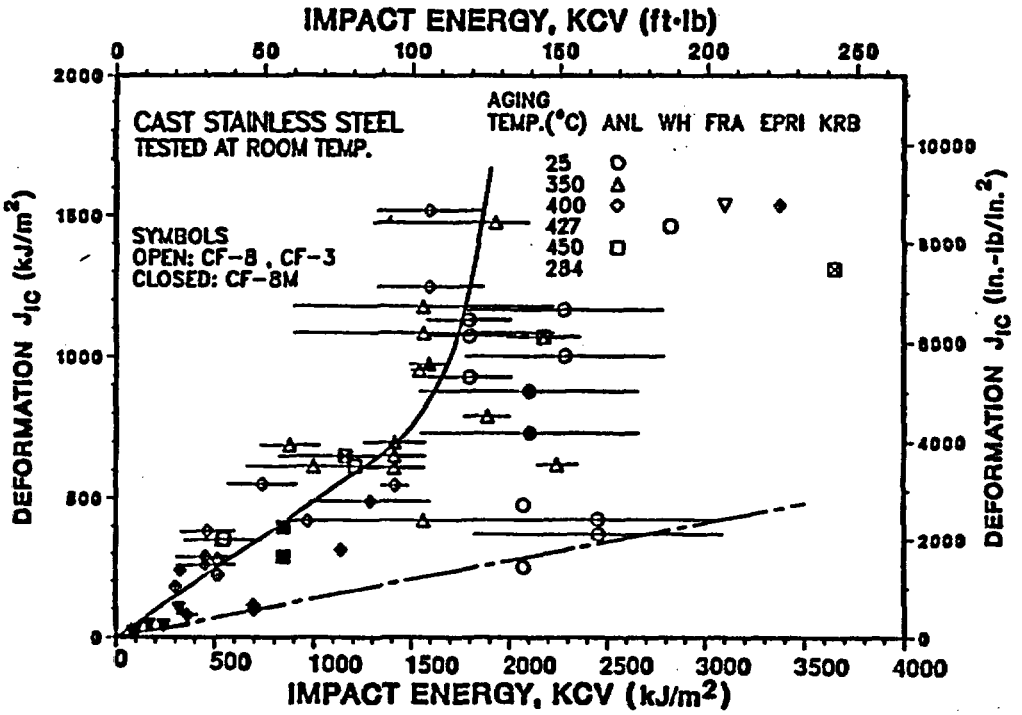

Figure 12. Correlation between room-temperature fracture toughness (J_{IC}) and impact energy for cast stainless steels.

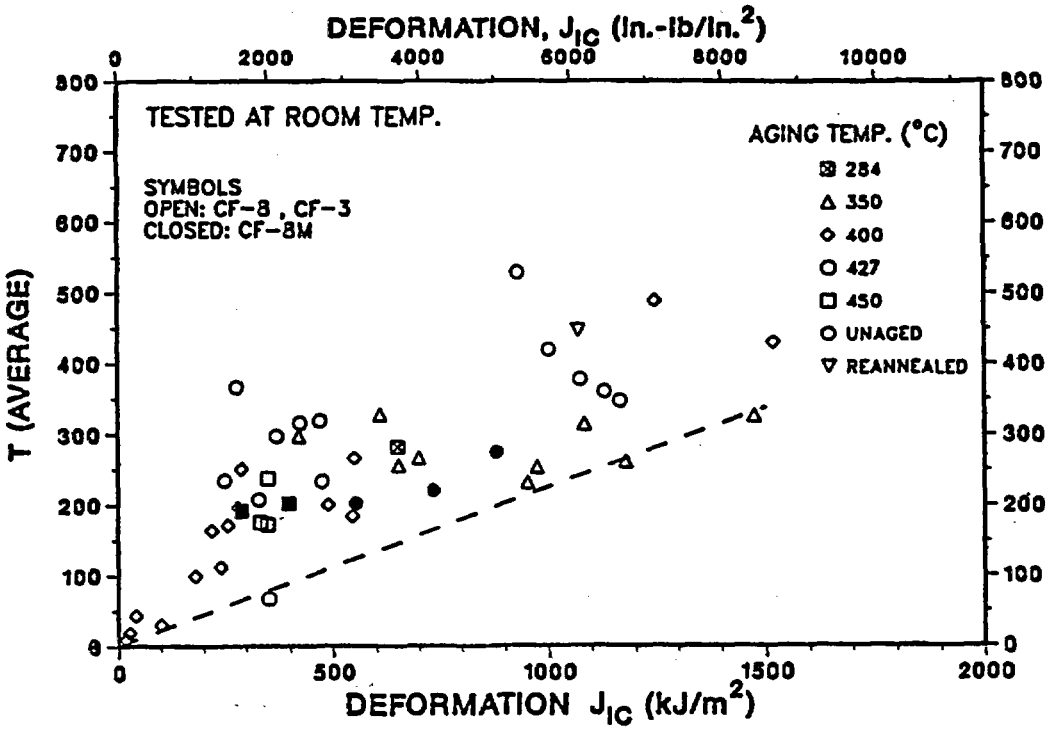

Figure 13. Correlation between room-temperature tearing modulus (T) and fracture toughness (J_{IC}) for cast stainless steels.

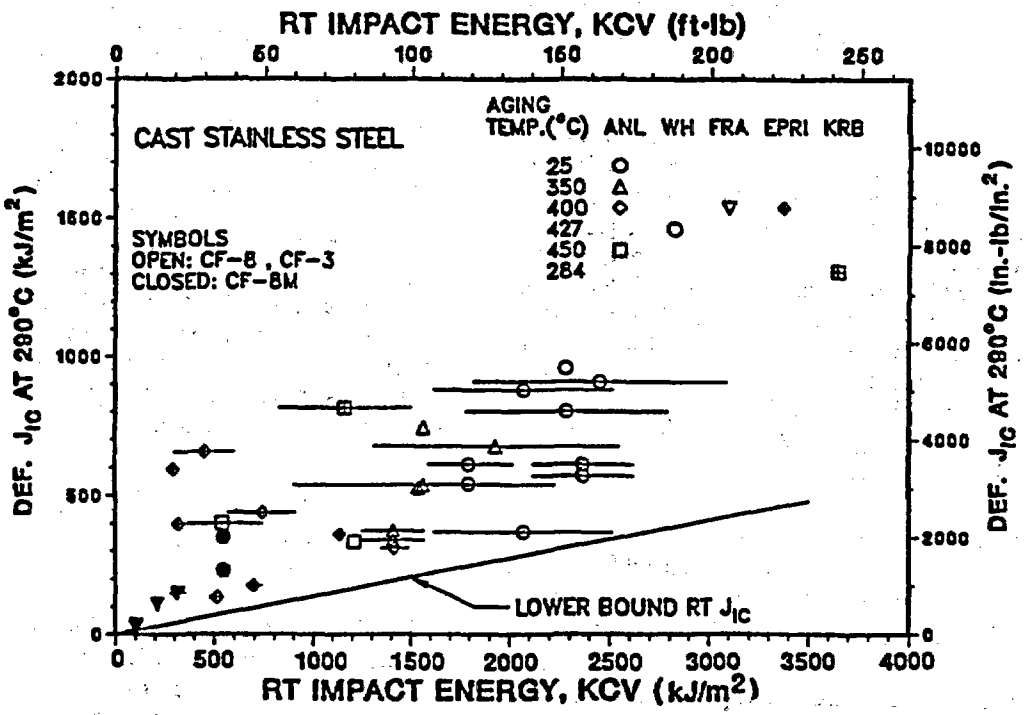

Figure 14. Correlation between the 290°C fracture toughness (J_{IC}) and room-temperature impact energy for cast stainless steels.

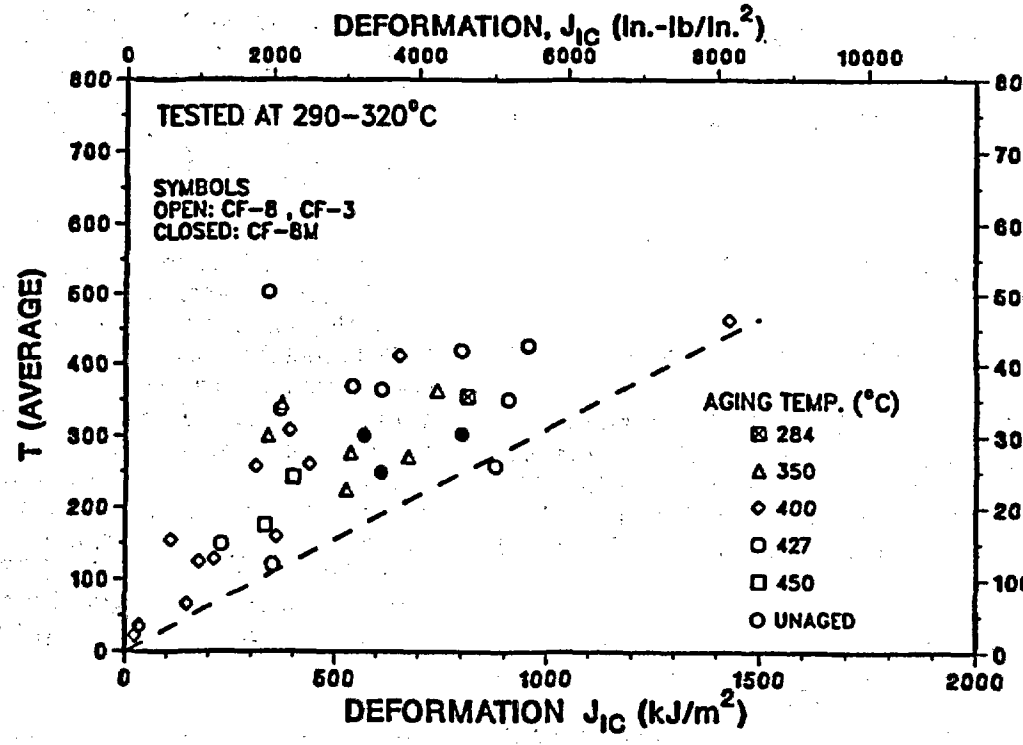

Figure 15. Correlation between the 290°C tearing modulus (T) and fracture toughness (J_{IC}) for cast stainless steels.

toughness and tearing modulus at temperatures lower than 290°C are needed for the pressurized thermal shock analysis of cast stainless steel components.

The correlations shown in Figures 12 and 14 may not be valid for higher values of J_{Ic}, because it is likely that many of the indicated J_{Ic} values do not satisfy the validity criteria of ASTM E 813, which requires that the thickness, B, and the uncracked ligament, b, of the test specimen be greater than 25 J_Q/s_f. J_Q is the conditional value of fracture toughness, and s_f is the flow stress, which is the average of the ultimate tensile strength and the 0.2% offset tensile yield strength. If these size conditions, plus the regression-line slope condition (see Paragraph 9.2 of ASTM E 813), are satisfied, then J_Q equals J_{Ic}.

Typical tensile properties (Chopra and Chung, 1987) of cast stainless steels that were aged for 9,980 h at 350°C (660°F) and tested at room temperature and at 288°C (550°F) yield s_f = 440 MPa at room temperature (RT) and 300 MPa at 288°C. The data shown in Figures 12 and 14 were developed from tests of 1T compact-type specimens, for which typically B = b = 25.4 mm. From this information, it is possible to estimate the maximum value of J_Q for which valid J_{Ic} values can be obtained, as follows:

$$J_Q(\text{maximum}) = 440 \times 25.4/25$$

$$= 447 \text{ kJ/m}^2 \text{ at RT} \qquad (6)$$

and

$$J_Q(\text{maximum}) = 300 \times 25.4/25$$

$$= 305 \text{ kJ/m}^2 \text{ at 288°C} . \qquad (7)$$

J_{Ic} values in Figure 12 and 14 that are greater than 447 and 305 kJ/m^2 at RT and 288°C (550°F), respectively, may not satisfy the validity criteria of ASTM E 813. Additional work should be performed to evaluate the validity of the J_{Ic} values plotted in Figures 12 and 14.

Based on fracture-mechanics evaluations of their cast stainless steel components, Framatome recommends that a lower-bound value of J_{Ic} equal to 100 kJ/m^2 be used for assessing those components.[a] This lower-bound value is specific to the cases analyzed by Framatome. Comparable lower-bound J_{Ic} values would have to be developed for other specific cases as they are evaluated, but it is instructive to use this value as an example in the present discussion. For the lower bound in Figure 12, a J_{Ic} value of 100 kJ/m^2 corresponds to a Charpy V-notch impact energy of about 735 kJ/m^2 at room temperature. Only a few of the experimental data reviewed in this report fall below the Framatome lower-bound value. However, for the long exposure times (greater than 40 years) associated with plant-license renewal, there is a concern that more materials may embrittle to the degree that their properties fall below this lower bound or that there may be specific cases where a more conservative lower-bound value of impact toughness is necessary. This needs to be determined by case-specific structural integrity assessments.

2.4 Tensile and Fatigue Properties

In addition to fracture-toughness properties, the tensile, fatigue-crack initiation, and fatigue-crack propagation properties of cast stainless steels are important for use in engineering evaluations of fitness for service. Typically, thermal aging increases the tensile ultimate and yield strengths and decreases the tensile ductility (Landerman and Bamford, 1978; and Chopera and Chung, 1987).[a] However, Chopra and Chung (1987) also report that a 12-year reactor-service exposure slightly decreased the tensile strength of a CF-8 pump cover plate. Overall, thermal aging does cause changes in tensile properties, but such changes do not appear to have a significant effect on the design-allowable strengths of cast stainless steels.

Landerman and Bamford (1978) reviewed the low-cycle fatigue-crack-growth properties of cast stainless steels. They found that the CF-8M stainless steel exhibited about the same fatigue-crack-growth resistance as comparable wrought alloys, and that aging at 427°C for 3000 h exhibited no significant effect on the fatigue-crack-growth resistance in either air or simulated PWR water environments. However, these results are only for aged CF-8M stainless steel. Many cast stainless steel components, including reactor coolant piping, are made of CF-8 and CF-8A stainless steels, and the fatigue-crack growth rates for these materials in a PWR environment may be significantly

a. Unpublished paper presented by G. Slama et al. at SMiRT Postconference Seminar 6 at Monterey, California, August 29-30, 1983.

different than that for CF–8M material, depending upon the carbon content. One possible explanation for this potentially different behavior is that chromium carbides may form at the ferrite–austenite interface in CF–8 and CF–8A materials at operating temperatures, whereas the presence of molybdenum prevents such formation in CF–8M stainless steel.[a] This explanation needs to be validated. If corrosion fatigue is a probable degradation mechanism for CF–8 and CF–8A stainless steels, accelerated aging at higher–than–operating temperatures would not be valid.

Slama et al.[b] evaluated both the low–cycle fatigue crack–initiation behavior and fatigue–crack–growth resistance of cast stainless steels at both room temperature and 320°C (610°F). They found that

a. Private communication with H. M. Chung, Argonne National Laboratory, April, 1990.

b. Unpublished paper presented by G. Slama et al. at SMiRT Postconference Seminar 6 at Monterey, California, August 29–30, 1983.

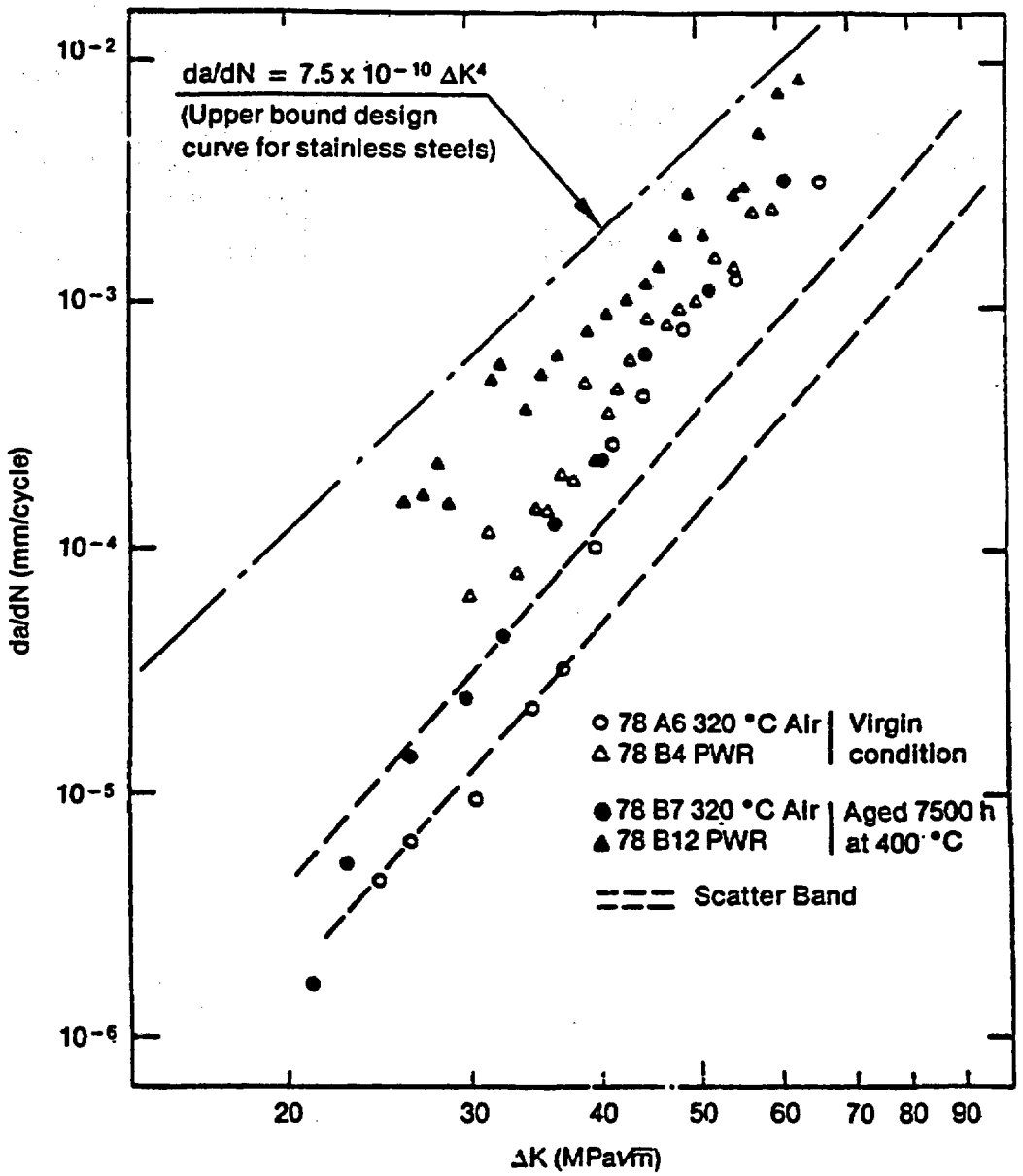

Figure 16. Fatigue crack growth rate of CF–8M stainless steel, in air and in PWR environment, at a cyclic frequency of 0.017 Hz (see footnote b).

thermal aging caused a small (10 to 15%) increase in cyclic yield strength, and, although one might expect reduced tensile ductility to reduce low-cycle fatigue resistance, they found no significant effect of thermal aging on low-cycle fatigue-crack-initiation resistance. Fatigue-crack-growth-rate resistance in air also was not significantly affected by thermal aging. However, as is illustrated in Figure 16, they found that fatigue-crack-growth rates for aged CF-8M stainless steel increased by as much as a factor of 10 when tested in a simulated PWR water environment, compared to testing in air at 320°C (610°F), but did not exceed the upper-bound design fatigue-crack-growth-rate curve for stainless steels.

Additional data for the fatigue crack initiation and growth in CF-8, CF-8A, and CF-8M stainless steel materials in LWR environments are needed. Data for high-cycle fatigue behavior of CF-8M material are needed because some cast stainless steel surge lines and elbows are subject to thermal stratification. Data for the fatigue behavior of irradiated cast stainless steel materials are needed because some reactor internals are made of these materials. No data are presently available for fatigue behavior of cast stainless steels in a BWR environment. The corrosion-fatigue behavior of aged cast stainless steel in a BWR environment needs to be evaluated.

In summary, thermal aging of cast stainless steels has been found to produce some increase in tensile strength and some degradation in known fatigue properties, but it may cause a significant degradation in fracture toughness. This degradation could impair the structural integrity of cast stainless steel components during long service. Thus, the fracture toughness and impact energy of thermally embrittled material are the most important items in evaluating the long-term structural integrity of cast stainless steel components (Bamford et al., 1987). In addition, degraded fatigue and stress-corrosion-cracking resistance, if any, should be taken into account in evaluating the integrity of cast stainless steel components.

3. INSERVICE INSPECTION OF COMPONENTS

Nondestructive examination (NDE) procedures are used to detect and characterize the nature of defects in cast stainless steel components. Application of NDE to cast stainless steel components is complicated because the material microstructure often contains a coarse, variable, and unpredictable combination of columnar and equiaxed grains (Egan et al., 1987; EPRI, 1986; Avioli, Jr., 1986; Gregory et al., 1986; Umino and Rao, 1984). Ultrasonic testing (UT) is preferred for the volumetric inservice inspection of many LWR components. However, conventional UT is not sufficiently reliable for cast stainless steel because coarse grains cause high attenuation and scattering that result in a low signal–to–noise ratio and make defect detection difficult. The noise level in cast stainless steel is significantly higher than that in wrought stainless steel. In addition, different grain structures in cast stainless steel introduce elastic anisotropy, which causes velocity variation and beam skewing and consequently inaccurate detection of the defect. Cast stainless steel is elastically isotopic if composed of equiaxed grains and the resulting variation in wave velocity with its propagation direction is small (2%), whereas cast stainless steel is elastically anisotropic if composed of columnar grains and the resulting variation in velocity with its propagation direction is large (as much as 100% for shear waves) (Kupperman et al., 1987). For these reasons, radiography normally is used for the NDE of cast stainless steel components, both during fabrication and during inservice inspection, especially for thick cast sections such as those used in pump bodies.

Radiography indicates the presence of a flaw, but, used alone, it cannot determine the depth of the flaw or whether the flaw is connected to the surface. For this reason, radiographic indications must be assumed to be a flaw of the most detrimental shape and location (Umino and Rao, 1984). Fracture–mechanics analysis indicates that the worst–case flaw will be a surface crack of 0.5 aspect (depth/length) ratio. Additional penetrant examinations can be performed to determine if the indication is actually a surface flaw. If the indication can be shown to be an imbedded flaw, then the stress intensity factor caused by such an imbedded flaw can be used in the fracture–mechanics analysis.

Use of radiography during inservice inspection is less practical and is less efficient than during fabrication. In some cases, structural restraints do not allow sufficient access for radiography. Therefore, both the NRC[a] and the nuclear industry (especially EPRI) (Avioli, Jr., 1986; Gregory et al., 1986; EPRI, 1986) have initiated research programs for the development of advanced UT methods to inspect cast stainless steel components. Advanced methods use low–frequency (longer wave length) transducer and short pulses, which enhance the signal–to–noise ratio and improve the capability to detect flaws. Two digital signal processing techniques, time and spatial averaging, can also provide a high degree of sensitivity and a high signal–to–noise ratio (Jeong and Ammirato, 1989; Shankar et al., 1988). The time averaging technique improves the presentation of data and makes them clearer and easier to interpret. The spatial averaging technique, which is similar to the synthetic aperture focusing technique (SAFT), reduces grain noise indications and, thus, enhances the signal–to–noise ratio for cracks larger than the average grain size. An additional difficulty in the inspection of statically cast components, such as pump casings, comes from rough surfaces and irregular surface contours, which cause poor transducer coupling with the component. For reliable examination, the surface condition needs to be improved by mechanical means such as grinding.

The effect of grain structure on the propagation of ultrasonic waves in cast stainless steel material has been studied to increase the accuracy of locating defects. Specially designed cast stainless steel specimens with cracks were tested to experimentally determine the effects of grain structure on wave propagation. These results are used to identify the grain structure in a cast stainless steel component, which is in turn used to compensate for the grain effect in UT examination to locate defects. Ultrasonic examinations were used to characterize grain structures in centrifugally cast stainless steel piping at the Vogtle power plant during preservice inspection.

Ultrasonic examinations were used to inspect welds and statically cast components, such as pump casings and elbows, at several domestic PWR plants (Jeong and Ammirato, 1989). The spatial averaging technique was used in these inspections to enhance the signal–to–noise ratio. The base metal of the hot–leg elbow at the Trojan plant was inspected because of a concern for high stresses. The concern was caused by the fact that several rupture constraints for the primary coolant

a. Private communication with M. S. Good, Battelle Pacific Northwest Laboratories, November 6, 1986.

piping were displaced from their original design positions. ASME Section XI inservice inspection requirements for cast stainless steel components do not include inspection of the base metal but include inspection of welds. However, the statically cast components are likely to have a larger number of fabrication defects than the welds, and, therefore, may be more susceptible to cracking. ASME Section XI inspection requirements for statically cast stainless steel components need to be reevaluated.

Double-probe search units, also called twin-crystal search units, were used to inspect PWR Type F pump casings (200-mm thick) at the Tihange 1 plant in Belgium. These units employ low-frequency (0.5 MHz) longitudinally polarized waves for enhancement of signal-to-noise ratio but are limited to a depth range from 10 to 60 mm (Dombret et al., 1990). Large-diameter (140-mm) focused transducers were used to examine down to a depth of 200 mm.

Advanced UT systems also show promise for the NDE of centrifugally cast stainless steel piping, but additional development and validation are needed before they can be used routinely for inservice inspections. An EPRI study (Gregory et al., 1986), using samples of centrifugally cast stainless steel pipe with weldments, evaluated the accuracy of the advanced UT methods. The signals appear to be satisfactory for crack detection. However, because of the type of microstructure, cracks were not always detected or consistently sized when the same regions were inspected from both sides of the pipe wall. Field studies at a PWR plant (prior to service) have evaluated the feasibility of using advanced UT systems to inspect centrifugally cast stainless steel pipe (Avioli, Jr., 1986). The results of that work indicate that advanced UT systems can be used to make measurements successfully in the field, but that additional development is needed to make the scanners adaptable to all of the various piping configurations that may be encountered. Another EPRI study has evaluated the use of Lamb waves, an ultrasonic surface wave technique to detect large-scale cracks (80% or greater through-wall cracks) in centrifugally cast piping (Georgetown University, 1988). Lamb waves are not as severely affected by grain structure as the conventional ultrasonic waves, and, therefore, experience less attenuation and lower noise levels. Development of a prototype search unit and a crack sizing capability for this technique are needed so that its use as an inservice inspection tool can be evaluated.

Use of the acoustic emission technique to detect crack growth in cast stainless steel components needs to be evaluated because of the difficulties with the radiography and UT examinations to detect flaws. Crack growth through the embrittled ferrite phase releases the elastically stored energy in the typical frequency range of 0.1 to 0.5 MHz.[a] The higher the degree of thermal embrittlement, the higher the crack velocity through the ferrite phase, and the amplitude of the resulting acoustic emission signal will be larger. If the crack growth in the embrittled cast stainless steel is through the ferrite phases, it will be composed of several small steps of brittle crack propagation and is most likely to be detected by the acoustic emission technique. Coarse grains of cast stainless steel material cause little scattering of the acoustic emission signal because the signal has a low frequency content (0.1 to 0.5 MHz); the corresponding wave length ranges from 30 to 6 mm, which exceeds the grain size.

The influence of thermal embrittlement of cast stainless steel on acoustic emission signals has not been investigated. However, the influence of another embrittlement mechanism, i.e., hydrogen embrittlement, has been investigated. In hydrogen embrittled material, the crack growth itself generates AE signals with amplitudes higher than 40 db above electronic noise. These signals are likely to be detected even under plant operational conditions.

---

a. Private communication with P. Jax, Bechtel/KWU Alliance, May 1990.

4. ASSESSMENT OF DEGREE OF MATERIAL EMBRITTLEMENT

For license renewal, one needs to be able to estimate the amount of thermal embrittlement that has occurred in cast stainless steel LWR components during past service and also the amount of embrittlement that is expected to occur during the license renewal period. The estimation techniques involve a combination of (a) analytical modeling of inservice degradation, (b) metallurgical evaluation methods, and (c) nondestructive testing. These three topics are addressed separately in the following subsections of this report.

4.1 Analytical Modeling of Inservice Degradation

The time–temperature aging parameter P, given previously by Equation (1), is the basis for a proposed model of inservice degradation caused by thermal embrittlement. The parameter, through Equation (2), is based on bulk chemical composition, but it does not directly account for the effects of ferrite volume fraction or ferrite spacing. However, because the ferrite volume fraction is related to composition, P indirectly incorporates the effect of ferrite volume fraction on thermal embrittlement. Also, as was pointed out previously, P does not completely correlate the effects of aging time and temperature with the measured changes in impact energy. However, P provides the best model that is currently available. With appropriate conservative assumptions, P can be used to estimate the amount of thermal embrittlement expected in LWR service, and as improved models are developed, those can be incorporated into the approach suggested below.

The lower–bound lines shown in Figures 5 through 7 are applicable to exposure temperatures of 400°C (750°F) or less and can be described by the following relation:

$$\log_{10}(\text{CVN}) = b_1 + b_2 P \quad \text{for } P \leq 4 \qquad (8a)$$

and

$$\log_{10}(\text{CVN}) = b_3 \quad \text{for } P > 4 \qquad (8b)$$

where CVN is the Charpy V–notch impact energy in kJ/m^2, P is the aging parameter of Equation (1), and b_1, b_2, and b_3 are material–dependent constants with the following values:

Alloy	b_1	b_2	b_3
CF–8M	3.412	–0.245	2.432
CF–8	3.30	–0.220	2.42
CF–3	3.310	–0.0954	2.928

Substituting Equation (1) into Equation (8) gives the following expression:

$$\log_{10}(\text{CVN}) = b_1 + b_2 \log_{10}\left\{ t/\exp[(Q/R)(1/T - 1/673)]\right\} \quad \text{for } P \leq 4 \qquad (9a)$$

$$\log_{10}(\text{CVN}) = b_3 \quad \text{for } P > 4 \; . \qquad (9b)$$

For a given alloy, chemical composition, exposure time, and exposure temperature, a lower–bound or minimum Charpy V–notch impact energy can be estimated using Equations (4) and (9).

Equation (9) can be used to estimate the range of potential CVN values as a function of exposure time at a specific temperature for CF–8M, CF–8, and CF–3 stainless steels. As mentioned, Chopra and Sather (1989) report that the correlation represented by Equation (4) was developed for observed values of Q between 75 and 240 kJ/mole. For the allowed compositions of these three stainless steels (see Table 3), all three could have values of Q between 75 and 240 kJ/mole. Thus, for purposes of illustration, these were assumed to be the minimum and maximum values of Q for a material in service and were used with Equation (9) to estimate lower–bound room–temperature Charpy values as a function of exposure time at 300°C (570°F), as presented in Figure 17.

Figure 17 shows that CF–3 is expected to be the least affected by aging, and that CF–8M and CF–8 are expected to be affected about the same and much more than CF–3. For the maximum Q of 240 kJ/mole, the saturation level (P = 4) is not expected to be reached within 100 years. For the minimum Q of 75 kJ/mole, the saturation level (P = 4) is expected to be reached within about 11.8 years. For the long–term exposure of CF–8 or CF–8M, the worst–case (minimum Q) room–temperature CVN value is predicted to be about 260 kJ/m^2; whereas the corresponding value for CF–3 is predicted to be high, equal to about 850 kJ/m^2.

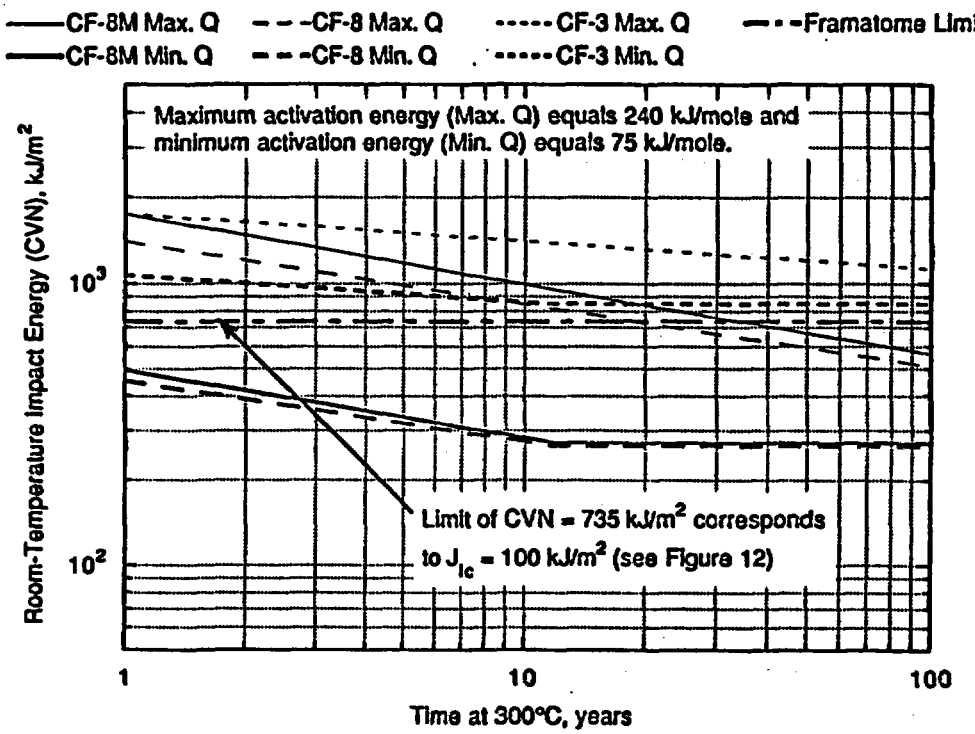

Figure 17. Predicted lower-bound Charpy-impact values for cast stainless steels as a function of aging time at 300°C (500°F).

The horizontal, chain-dashed line in Figure 17 at 735 kJ/m^2 corresponds to a lower-bound J_{Ic} value of 100 kJ/m^2 mentioned by Slama et al. of Framatome for possible use in safety assessment of cast stainless steel components. Only the CF-3 alloy is predicted to satisfy this limit. Most of the CF-8 and CF-8M compositions are predicted to fall below this limit after 10 to 20 years of aging.

The wide spread between the maximum and minimum lines in Figure 17 further emphasizes the need for research to better define the value of Q at temperatures of 300°C or less discussed previously. If the value of Q at these lower temperatures is close to 250 kJ/mole, as was suggested by Bonnet et al. (1990), the rate of embrittlement would be expected to be close to the lines for maximum Q in Figure 17.

Figure 17 could be used to estimate the degree of embrittlement of a cast material of unknown composition. However, it is recommended that the actual composition be used to compute Q. Then, if the computed Q value is between 75 and 240 kJ/mole, a plot such as that shown in Figure 17 can be prepared for that specific material and the temperature(s) of interest.

4.2 Metallurgical Evaluation Methods

Metallurgical evaluation methods currently provide the best approach for quantifying thermal embrittlement in cast stainless steel components that have been in service. These methods can involve either nondestructive measurements and examinations or destructive tests and examinations of small samples that have been removed from components. When samples are taken from a component, they must be removed in a manner such that there is no functional damage to the component or such that the component can be acceptably repaired. The metallurgical evaluation methods either characterize the microstructure to generate data for estimating the degree of embrittlement using degradation models or characterize mechanical properties by testing subsized or miniature samples.

4.2.1 Microstructure Characterization. The volume fraction of ferrite in cast stainless steel components needs to be determined because it is the primary microstructural parameter controlling thermal embrittlement. If the ferrite content is below 10%, the potential for material degradation is likely to be low. For ferrite levels between 10 and 15%, the potential for material degradation is likely to be moderate.

Significant degradation may take place when the ferrite level exceeds 15%.

The amount of ferrite can be estimated from the measured bulk chemical composition of the material. Procedures for estimating ferrite content have been reviewed by Leger (1982) and Aubrey et al. (1982). All of these procedures are based on calculating a chromium equivalent value, Cr_e, and a nickel equivalent value, Ni_e, and using these equivalent values to compute a volume percent ferrite content, %F. The empirical formulas for computing these values have been developed from correlations of experimental data. Aubrey et al. (1982) used linear regression analysis to evaluate four different ferrite estimation formulas for an extensive database of information on CF–3, CF–8, and CF–8M stainless steels and found that the following relationship gave the best overall results:

$$\%F = 100.30\,(Cr_e/Ni_e)^2 - 170.72\,(Cr_e/Ni_e) + 74.22 \qquad (10)$$

where

$$CR_e = \%Cr + 1.21(\%Mo) + 0.48(\%Si) - 4.99 \qquad (11)$$

and

$$Ni_e = \%Ni + 0.11(\%Mn) - 0.0086(\%Mn)^2 + 18.4\,(\%N) + 24.5(\%C) + 2.77\,. + 2.77\,. \qquad (12)$$

Thus, if the bulk chemical composition of a cast stainless steel component is known or measured, Equations (10), (11) , and (12) can be used to estimate its ferrite content.

Bonnet et al. (1990) have developed the following, slightly different method for predicting the amount of ferrite from the chemical composition:

$$\%F = [21.8(Cr_e/Ni_e)^2 - 5.96(Cr_e/Ni_e) + 3.39][400]/[1500 - T]$$

where

T = temperature of the final heat treatment in °C

Cr_e = %Cr + %Mo + 0.65 (%Si) – 17.6

and

Ni_e = %Ni + 0.08 (%Mn) + 8.3 (%N) + 20 (%C) – 5.18 .

This method is similar to the one defined by Equations (10), (11), and (12), except that it has different values of the coefficients for the terms and includes an additional term to account for the temperature of the final heat treatment. Bonnet et al. (1990) report an accuracy of ±3% ferrite for their method, which is about twice as good as the ±6% ferrite accuracy cited by Aubrey et al. for their method.

In many cases, the final heat treating temperature is not known, and the method of Bonnet et al. cannot be applied. When the final heat treating temperatures are known, the resulting correction factor, [400]/[1500 – T], could be as large as 25%. For example, in the work of Aubrey et al. the final heat treating temperatures ranged from 1093 to 1177°C (2000 to 2150°F), which gives corresponding values of the temperature correction factor of 0.98 to 1.24. Thus, it may be worthwhile in future research to evaluate the method of Bonnet et al. for typical castings produced in the United States.

Leger (1982) found that ferrite content also increases as section thickness increases, as is shown by the data for CF–8M stainless steel in Figure 18. The ferrite content as a function of thickness appears to saturate (reach a constant value) at section thicknesses greater than approximately 45 mm (1.77 in.). Therefore, using the data for the thicker castings would provide conservative (larger than actually expected) estimates of ferrite content for thinner castings. The work of Aubrey et al. (1982) was for castings thicker than 25 mm (0.98 in.), so Equations (10), (11), and (12) probably provide reasonable predictions for thick–section castings.

Equations (10), (11), and (12) were used to estimate the ferrite content of the 45–mm thick samples of CF–8M that were evaluated by Leger (1982) and of the 100–mm (3.94 in.) thick samples of CF–8 and CF–8M that were discussed previously (see Figure 4). Figure 19 shows that there was a good correlation between predicted and measured ferrite content for these data. The solid line indicates the mean correlation; the dotted and dashed lines indicate the upper and lower limits,

respectively, which are plus and minus two times the standard error [estimated at 3.03, as reported by Aubrey et al. (1982)] from the mean correlation, respectively.

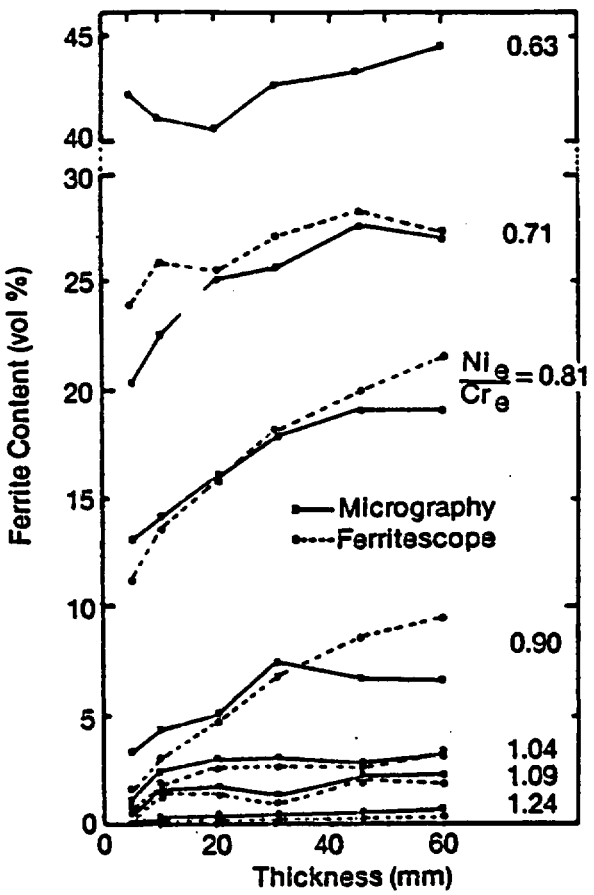

Figure 18. Ferrite content of CF–8M castings as a function of section thickness (Leger, 1982).

In order to make a reasonably conservative estimate of the ferrite content, one would add 6.06 to the value calculated using Equation (10) for comparison with acceptable ferrite levels. Thus, for the adjusted ferrite content to not exceed an upper–limit ferrite content of 15%, the mean ferrite content calculated using Equation (10) should not exceed 8.94. This value is only slightly greater than the minimum ferrite level of 8% that is recommended to avoid sensitization during welding (Hazelton, 1988). Furthermore, if one adds 6.06 to 8 to account for the expected uncertainty, the minimum would be 14.06%. This ~5% overlap in desirable minimum and maximum levels occurs because of the uncertainty associated with calculating ferrite content from composition. Therefore, the calculation of ferrite levels from chemical composition provides only approximate guidance for the assessment of stainless steel castings and is of limited use in quantifying thermal embrittlement.

Recent results indicate that ferrite spacing, as well as ferrite content, may influence the degree of thermal embrittlement (Chopra and Chung, 1986b, 1987b, 1989a, 1989b). Procedures for estimating the ferrite spacing in a cast stainless steel component are not available, but, as discussed previously, Chopra and Chung (1990a) recommend that a value of ~180 μm be assumed as a worst–case condition if the actual ferrite spacing has not been measured. Since the ferrite spacing is a significant factor in the Φ parameter, which correlates with the minimum Charpy impact energy expected after long–term exposure, it would be useful to develop a procedure for estimating the ferrite spacing in stainless steel castings.

Measuring ferrite content is an alternative to estimating it. If a material sample can be removed from the component, then quantitative metallographic procedures can be used to measure the ferrite content (Leger, 1982; Aubrey et al., 1982). The procedures typically employ either computerized image analysis or manual point–counting techniques. The average ferrite spacing also could be measured during metallographic examination. Material sampling must be performed carefully to ensure that the regions examined represent the bulk material. Because sample removal often may be limited to exterior or interior regions, quantification of the ferrite volume and spacing within the wall of the component is difficult.

The above metallographic measurements can be made on surface replicas of selected areas of a component in the field. Metallographic replication has been developed as a viable NDE tool (Neubauer and Wedel, 1983); Auerkari, 1983; Viswanathan, 1985; Harth and Sherlock, 1985; Henry and Ellis, 1983; Hilton and Steakley, 1986; Janiszewski et al., 1986; Takigawa et al., 1986; Masuyama et al., 1985), and ASTM Emergency Standard ES–12 for field replication has been developed.[a] Prototype replication equipment has been used to remotely examine the inside surface of steam–turbine rotors (Takigawa et al., 1986) and to inspect steam–generator tubes (Padden, 1983; Padden and Daniels, 1976, 1981). Replicas must be made at ambient temperature during an outage and at surface locations that are accessible. As with sample removal, judicious selection of the areas to be replicated is necessary.

a. From a presentation by J. DeLong at the ASTM–ASME–MPCJ–1 Workshop at the ASME Winter Annual Meeting, Anaheim, December 9, 1986.

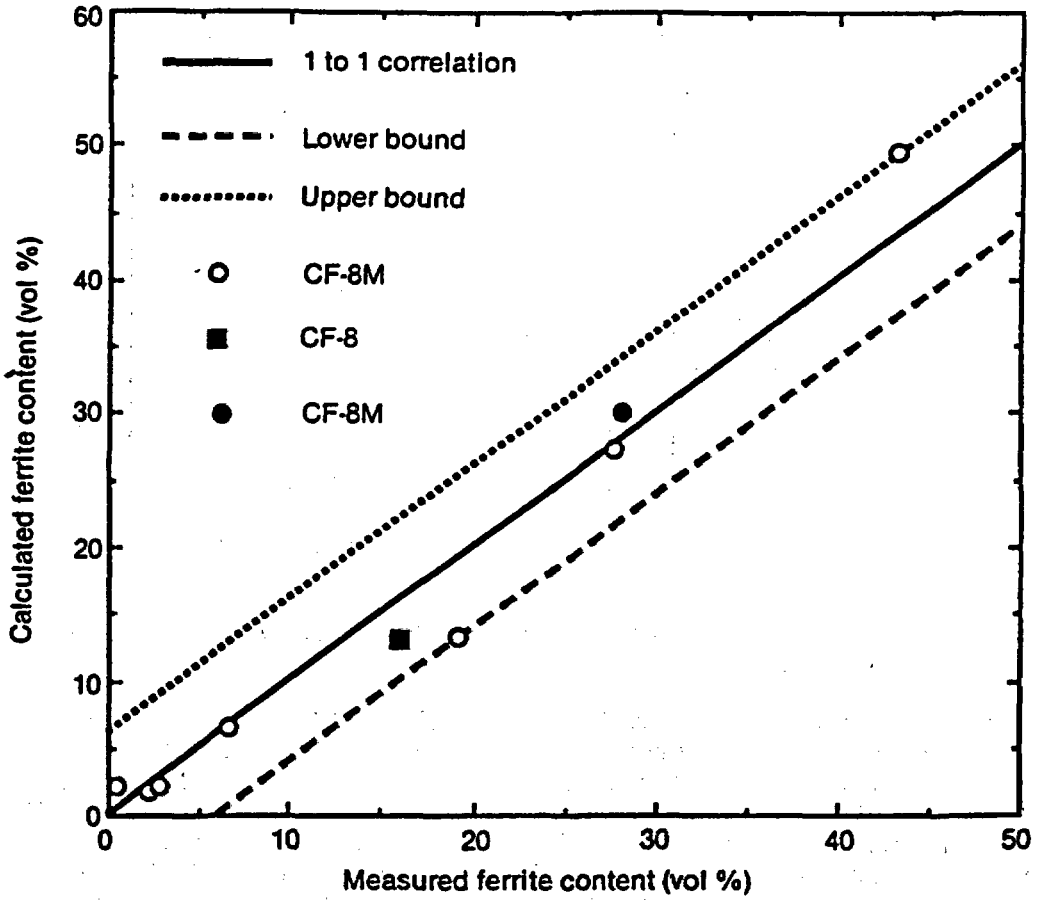

Figure 19. Comparison of ferrite content predicted from chemical composition with measured ferrite content using Model 1 of Aubrey et al. (1982) (CF-8M data from Leger, 1982; other data from Aubrey et al., 1982).

Because the ferrite phase is significantly more magnetic than the austenite phase, ferrite content can be measured by instruments that measure the magnetic properties of the stainless steel. Field measurements of ferrite content, based on magnetic properties, can be made using a Ferritescope (Leger, 1982; Aubrey et al., 1982). This instrument can be used in the field to measure ferrite levels up to 30% and has been demonstrated to produce reliable measurements for samples with section sizes ranging from 27 to 152 mm (1.06 to 6.0 in.) (Aubrey et al., 1982). Figure 20 shows that a good correlation between ferrite content measured using the Ferritescope and using a metallographic point-counting method can be obtained. This method appears promising, but field validation tests on representative LWR cast stainless steel components are necessary before it can be used routinely during inservice inspections. Section III of the ASME Boiler and Pressure Vessel Code now permits the use of magnetic measuring instruments for determining the ferrite levels in welds.

Bonnet et al. report that the saturation magnetic method (using a Sigmametre) provides the most reliable experimental technique for measuring the amount of ferrite. This method is somewhat different than the magneto-induction method on which the Ferritescope is based. Curtis and Sherwin (1961) discuss using the saturation magnetic method to measure the ferrite content of stainless steel welds. Either type of magnetic measurement method should provide reasonable measurements of ferrite amount if it is properly calibrated and used by a qualified operator.

Factors other than the bulk chemical composition and ferrite content and distribution in stainless steel castings may play an important role in thermal embrittlement. For example, as was shown previously (see Table 5), the chemical composition of the ferrite regions is significantly different from that of the austenite regions in these alloys. The partitioning of the

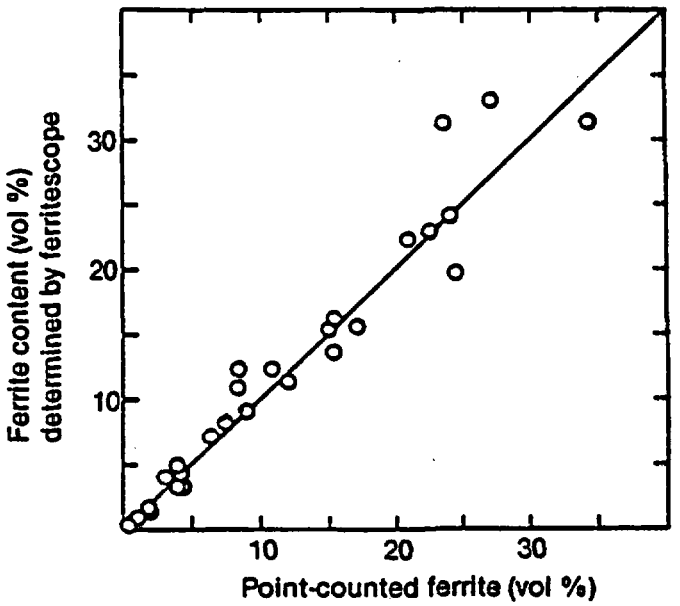

Figure 20. Comparison of ferrite content measured using a ferritescope with that determined metallographically by a point-count procedure.

ferrite-promoting elements to the ferrite phase may affect the amount of thermal embrittlement. If such an effect were found in future studies, a correlation between local composition and the degree of thermal embrittlement might be developed. Such a correlation might be useful in the future development of alloy compositions that would be resistant to partitioning during casting and to subsequent embrittlement during service at LWR operating temperatures.

4.2.2 Testing of Miniature Samples. Measuring the mechanical properties of small samples removed from stainless steel castings is another potential method for quantifying the degree of thermal embrittlement caused by service exposure. Two approaches could be used. Fracture toughness could be measured directly using subsized specimens. Alternatively, impact energy, tensile strength, or indentation resistance could be measured and used to estimate fracture toughness if appropriate correlations were available. Direct measurement of fracture toughness usually is more costly and normally requires larger samples than the indirect measurements. However, the direct measurements are generally more reliable than the indirect ones.

There has been a great deal of recent interest in the testing of subsized specimens to measure mechanical properties (Jaske et al., 1986; Manahan, 1981; Haggag et al., 1985; Misawa and Hamaguchi, 1986; ASTM, 1986; Huang, 1986; Lucas et al. 1986; Corwin and Hougland, 1986; McConnell et al., 1986). Much of this work has been motivated by the need to measure the properties of irradiated materials. For example, the ASTM special technical publication (ASTM 1986) includes 21 papers of the ASTM Symposium on the Use of Nonstandard Subsized Specimens for Irradiated Testing. These past studies included the comparative testing of standard-sized and subsized specimens of reactor pressure vessel steels and wrought austenitic stainless steels, but they did not include testing of the cast CF-8, CF-8M, and CF-3 stainless steels. Such testing is needed to validate the use of subsized specimens for these materials. Results of the past evaluations of subsized specimens do provide guidance for estimating the minimum specimen size that would be expected to yield valid measurements of J_{Ic}.

Experience indicates that the minimum specimen dimension should be at least five to ten times the significant microstructural feature (Jaske et al., 1986),[a] which for the cast stainless steels may be either the grain size or the ferrite spacing. Experimental studies are needed to establish what significant microstructural feature controls fracture toughness in cast stainless steels. Values of grain size and ferrite spacing are usually larger for heavy-section castings than for thin-section castings. If, for example, ferrite spacing is the significant feature, the minimum specimen dimension would range from about 0.25 to 2 mm, which

a. A. R. Rosenfield, unpublished research results, Battelle, Columbus, Ohio, 1985.

corresponds to typical ferrite spacing values that range from 50 to 200 μm (Chopra and Chung, 1987).

As was discussed previously, ASTM E 813 requires that the thickness, B, and the uncracked ligament, b, of a test specimen be greater than $25J_Q/s_f$, where J_Q is the conditional value of fracture toughness, and s_f is the flow stress, which is the average of the ultimate tensile strength and the 0.2% offset tensile yield strength. If these size conditions, plus the regression-line slope condition (see Paragraph 9.2 of ASTM E 813), are satisfied, then J_Q equals J_{Ic}.

Typical tensile properties (Chopra and Chung, 1987) of cast stainless steels that were aged for 9,980 h at 350°C (660°F) and tested at room temperature and at 288°C (550°F) can be used to estimate the minimum values of B and b that would be required to obtain valid J_{Ic} values. For example, if $J_{Ic} = 250$ kJ/m^2, which Figures 12 and 14 show is a fracture toughness value that could be expected for thermally embrittled cast stainless steel, and $s_f = 440$ MPa (64 ksi) at room temperature and 300 MPa (44 ksi) at 288°C (550°F), then

B, b (minimum) = 25 (0.25/0.44) = 14.2 mm at room temperature

and

B, b (minimum) = 25 (0.25/0.30) = 20.8 mm at 288°C.

If

$J_{Ic} = 100$ kJ/m^2, which is the lower bound used by Framatome[a]

then

B, b (minimum) = 25 (0.10/0.44) = 5.68 mm at room temperature

and

B, b (minimum) = 25 (0.10/0.30) = 8.33 mm at 288°C.

Thus, because even severely embrittled cast stainless steels have relatively high fracture toughness, fairly large specimens, rather than subsized ones, are needed for measuring their J_{Ic} values.

One property that could be measured on small material samples is microhardness of the ferrite phase. Recent research has shown that the Vickers hardness number of the ferrite phase increased from 260 in unaged material to 377 in aged material from a CF-8 casting (Chopra and Chung, 1987). It may be possible to establish a correlation between the hardness of the ferrite phase and the amount of thermal embrittlement. The correlation would have to take into account the effect of ferrite volume fraction and ferrite spacing, as discussed previously. Future research is needed to evaluate the potential for developing this type of microhardness-embrittlement correlation.

4.3 Use of Ultrasonic Testing to Characterize Materials

Use of ultrasonic techniques is being developed to quantify material embrittlement. Both Swanson (1981) and Vary (1976) have found correlations between ultrasonic attenuation and the fracture toughness of wrought low-alloy steels. Their measurements were made on well-documented samples under carefully controlled conditions in the laboratory. Similar studies have not been performed on cast stainless steels, and the work has not been extended to the field measurement of fracture toughness on components. Thus, extensive research and development work will probably be necessary before ultrasonic measurement methods can be used to quantify embrittlement in cast stainless steels.

a. Unpublished paper presented by G. Slama et al., at SMiRT Postconference 6 at Monterey, California, August 29–30, 1983.

5. WELD–REPAIR PROCEDURES

If inservice NDE reveals that defects are present in a cast stainless steel component, the possibility of weld–repairing that defect may be considered. CF–8, CF–8M, and CF–3 stainless steels are readily welded. Welding is routinely used to repair defects that may be found in castings of these alloys during component fabrication. The major concerns with inservice repairs are that access may be limited and that thermal embrittlement may affect weldability. The former item is common to inservice repairs of any alloy, while the latter item is unique to the cast stainless steels.

The procedures used for weld–repair of statically cast components during manufacturing have been reviewed elsewhere (Egan et al., 1987); a brief review of the standard procedures[a] developed for repair welding during the fabrication of centrifugally cast stainless steel pipe is presented here. After the pipe is cast and excess material is machined from the outside and inside surfaces, the pipe is fully radiographed to identify major and minor defects, in accordance with the ASME Code. The locations of all those defects are mapped and recorded for future reference. The defects are removed or reduced to an acceptable size by grinding or thermal gouging, with the final metal being removed by grinding using an aluminum oxide or silicon carbide wheel. The repair area is dye penetrant inspected and thoroughly cleaned with organic solvents before welding.

Welding procedures and welders are qualified as specified by the ASME Code (Group P–8). Welding is performed using the manual shielded metal–arc process and Type 316 weld rods that produce at least 7% ferrite in the weld metal. The minimum preheat is 56°C (133°F); no postweld heat treatment is employed, and the interpass temperature is kept below 177°C (350°F) for multiple passes. Welding current is maintained as low as possible, travel speed is maintained as high as possible, and stringer beads are used. After completion, all weld repairs are dye–penetrant inspected, and major repairs also are radiographed.

There should be no major problem in developing and qualifying similar weld–repair procedures for field use on components that have been in service, provided that the defect is local. For example, if a fatigue crack were found to have developed at a local geometric discontinuity in a component, then it would be feasible to consider a repair; but if fatigue damage were found to be significant throughout a component, a repair probably would not be feasible. In repair welding, care must be taken to minimize the introduction of residual stresses. On the other hand, postweld heat treatment is impractical in most cases, and when it is used, it could produce sensitized regions near the ends of the heat–treated area. For major repairs, it is likely that specific procedures will have to be developed and qualified on a case–by–case basis.

If repair welding is considered to be a viable option for license extension, research is needed to evaluate any problems that might be encountered in the welding of thermally embrittled material. For example, it might be found that thermally embrittled material is more susceptible to weld cracking than new material. Because the embrittlement mechanism is different for aging at temperatures greater than 400°C (750°F) than for aging at temperatures less than 350°C (660°F), the research should concentrate on the welding of materials that have been aged for long times at 350°C or less. Studies using samples that have been removed from actual LWR service would be particularly appropriate. Results of this type of research would provide guidance for the development and qualification of weld–repair procedures for cast stainless steel LWR components.

---

a. E. G. Kay, Sandusky Foundry & Machine Company, personal communication of unpublished information, October 1986.

6. LIFE ASSESSMENT PROCEDURE

There are two basic approaches to maximizing the structural integrity of LWR components for operation during and beyond the original license period. First, one can evaluate the current condition of a component, estimate its remaining safe life, and decide to repair or replace it only when there is cause to do so. This approach is employed widely to critical structural components whose failure would impact safety and whose unnecessary replacement would be extremely costly. A second approach would be to arbitrarily replace a component after some specified service life without attempting to determine its current condition. This method is applied to critical structural components whose failure would impact safety and whose replacement is easier and less costly than evaluating their current condition. For most cast stainless steel LWR components that are subject to the possibility of thermal embrittlement during long-term service, the second approach is undesirable because of an unfavorable cost/benefit ratio; thus, the first approach is the most reasonable one.

Figure 21 presents a generic procedure for aging and license renewal evaluations of LWR cast stainless steel components. Nine major steps are listed.

The first step is to review all of the design, fabrication, and construction records related to the components being evaluated. Some of the items listed in Step 1 may not be available. Those items should be identified, and plans to obtain them during the next inservice inspection (ISI) should be developed, if possible. In cases where it is not possible to obtain case-specific data for austenitic stainless steel products (e.g., impact and fracture toughness data are not required by *Section III of the ASME Boiler and Pressure Vessel Code*), worst-case data should be obtained from handbooks, technical literature, and industrial experience. The information collected in Step 1 should be stored for easy retrieval and reference in the future.

All of the ISI records for the components are reviewed in the second step. The information on defect indications and locations and maximum undetected flaw sizes is needed for the fracture mechanics evaluation (Step 4). The chemical compositions of the materials should be verified by measurements on the components. Essential information (such as size and location of flaws in the base metal) not being obtained during the current ISI programs should be obtained during future ISI programs. In many cases, key locations are not accessible to ISI, so the original records must be used with appropriate factors applied to account for uncertainty.

The third step is to review all of the data on operating history. The operating temperature is needed to evaluate the degree of thermal embrittlement, and data on loadings and cyclic operations are needed to help estimate the amount of crack propagation that might have occurred or might occur in the future. Indications of past problems may help point out areas that should be evaluated in Steps 4 and 5.

A fatigue and fracture-mechanics evaluation is performed in the fourth step. The locations and sizes of the existing flaws are identified from the ISI records. Simplified, conservative loadings are estimated from a review of the operating history. Stress analyses are performed to identify regions of the highest stress, and the stress history at the flaw locations is estimated. If the review of operating history reveals that certain loads were not included in the original design, revised calculations for the ASME Section III cumulative fatigue usage factors are made. Crack-propagation analysis is performed to estimate the maximum possible defect size at the end of the next operating period (EONOP). Finally, the minimum required fracture toughness corresponding to the worst-flaw size at the EONOP are determined.

The fatigue and fracture-mechanics evaluation performed in the fourth step is conservative because it assumes that the flaws in the cast stainless steel components are crack-like. This assumption is made because the current inservice inspection methods are not capable of completely characterizing the flaws. If an emerging inservice inspection method can positively identify that a given flaw is not crack-like, then a fatigue-crack initiation analysis would precede the crack propagation analysis. In such a fatigue analysis, an effective stress concentration factor is computed for the flaw (Hertzberg, 1983), and then the usage factor at EONOP is determined. If the usage factor is greater than 1.0, it is assumed that a crack will be initiated at the given flaw before EONOP; in this case, a crack propagation analysis would be needed.

In the fifth step, the material condition of the component is assessed to determine the minimum expected fracture toughness at EONOP. Three techniques can be employed to assess the degree of thermal embrittlement of a cast stainless steel component, as discussed in Section 4. The first technique uses the simplified

Figure 21. Generic procedure for the evaluation of LWR cast stainless steel components.

---

1. Collect and review design, fabrication, and construction records
   - 1.1 Design drawings and specifications
   - 1.2 Measure chemical composition of material
   - 1.3 All available mechanical properties for original material
     - 1.3.1 Tensile: ultimate, yield, elongation, reduction of area
     - 1.3.2 Impact: energy versus temperature, fracture appearance
     - 1.3.3 Fracture toughness
     - 1.3.4 Fatigue strength
     - 1.3.5 Fatigue–crack propagation behavior
   - 1.4 ASME Section III cumulative fatigue usage factors
   - 1.5 As–built drawings and dimensions
   - 1.6 Name, location, and date of fabrication
   - 1.7 Field installation procedures
   - 1.8 Type, location, and repair procedure for all casting defects
   - 1.9 Number, location, type, and heat treatment of welds
2. Review inservice inspection (ISI) records
   - 2.1 Location of inspected regions
     - 2.1.1 Were all welds inspected?
     - 2.1.2 Was base metal inspected?
     - 2.1.3 Were regions of high incidence of weld–repair during fabrication inspected?
   - 2.2 Nature, size, distribution, and disposition of indications (if any)
   - 2.3 Estimate maximum undetected flaw size based on ISI procedures
   - 2.4 Measurements of chemical composition (if any)
   - 2.5 Other information
3. Review operating history
   - 3.1 Hours of operation
   - 3.2 Number of start/stop cycles
   - 3.3 Number of major load swings
   - 3.4 Number of upsets
   - 3.5 Temperature
   - 3.6 Pressure
   - 3.7 Records of any past problems related to the component
4. Perform fatigue and fracture mechanics evaluation
   - 4.1 Identify size and locations of existing flaws from ISI records

Figure 21. Generic procedure for the evaluation of LWR cast stainless steel components. (Continued.)

- 4.2 Estimate simplified, conservative loadings from review of operating history
- 4.3 Perform stress analysis of component
  - 4.3.1 Identify regions of highest stress
  - 4.3.2 Estimate stress history at potential locations of flaws
- 4.4 Update ASME Section III cumulative fatigue usage factors, if design basis violated
- 4.5 Compute possible flaw growth (if any) during next operating period
- 4.6 Compute the minimum required fracture toughness and worst-case flaw size at the end of next operating period (EONOP)

5. Assess material condition
   - 5.1 Use simplified analytical model
     - 5.1.1 Use composition and maximum operating temperature to estimate lower-bound Charpy V-notch impact energy value at EONOP
     - 5.1.2 Or use composition, ferrite content, and ferrite spacing to estimate minimum Charpy V-notch impact energy at long life
     - 5.1.3 Estimate lower-bound fracture toughness at EONOP from fracture toughness versus impact energy correlation
   - 5.2 Assess ferrite content
     - 5.2.1 Calculate upper bound ferrite content from composition
     - 5.2.2. Measure ferrite content
       Metallographic sample from component
       Surface replication of component
       Ferritescope
     - 5.2.3 Use guidelines to estimate fracture toughness at EONOP
   - 5.3 Measure properties of small samples from component
     - 5.3.1 Fracture toughness testing
     - 5.3.2 Charpy testing
     - 5.3.3 Microhardness correlation
     - 5.3.4 Use simplified analytical model to estimate fracture toughness at EONOP

6. Evaluate component integrity at EONOP
   - 6.1 Compare the minimum required fracture toughness at EONOP with the corresponding estimated lower-bound value
     - 6.1.1 Is the minimum required fracture toughness smaller than the estimated lower-bound value by an acceptable margin?
     - 6.1.2 Estimate critical flaw size at EONOP
     - 6.1.3 Is critical flaw size safely detectable?
   - 6.2 Evaluate the potential for leak-before-break (LBB) to occur.

Figure 21. Generic procedure for the evaluation of LWR cast stainless steel components. (Continued.)

- 6.2.1 Is critical flaw size less than the wall thickness?
- 6.2.2 Will a through–wall crack produce a safely detectable leak before it reaches a critical size?

7. Establish action to be taken
   - 7.1 Continued operation to EONOP if acceptable safety margins are present
   - 7.2 Determine if repair procedures are needed
   - 7.3 Determine if replacement is needed.

8. Establish plan for next ISI
   - 8.1 Determine extent of inspection required
     - 8.1.1 Consider areas of high stress
     - 8.1.2 Consider areas where defects are most likely to exist
     - 8.1.3 Consider areas where weld repairs have been made
     - 8.1.4 Consider areas where temperature is the highest
     - 8.1.5 Consider areas where cumulative fatigue usage factors are high
     - 8.1.6 Consider areas where a flaw may grow by fatigue loading
     - 8.1.7 Consider areas where IGSCC may occur: welds with less than 8% ferrite
   - 8.2 Determine next inspection interval
     - 8.2.1 Use information on worst–case flaw size and crack–growth rate from Step 4 and on critical flaw size from Step 6
     - 8.2.2 Compute expected remaining safe life
     - 8.2.3 Set interval for next inspection at lesser of predetermined fraction (e.g., 1/4) of remaining safe life, or 10 years
   - 8.3 Develop a thermal–embrittlement surveillance program
     - 8.3.1 Make Charpy V–notch or fracture–toughness specimens of archival material
     - 8.3.2 Use both base metal and weld metal
     - 8.3.3 Expose the specimens at temperatures that lead the embrittlement rate of components by a factor of 1.5 to 3
     - 8.3.4 Evaluate selected samples at 5–year intervals to assess
       Rate of embrittlement (change in impact energy or fracture toughness)
       Degree of embrittlement (value of impact energy or fracture toughness)

9. Re–evaluate component(s)
   - 9.1 Perform as required
   - 9.2 Return to Step 2 of procedure

analytical model expressed by Equations (4) and (9) to estimate the minimum Charpy V-notch impact energy value at EONOP, or the Φ parameter of Equation (5) to estimate the minimum Charpy V-notch impact energy after long-term aging. Then, using a J_{Ic} (fracture toughness) versus CVN correlation, minimum J_{Ic} is estimated. The second technique is based on either calculating or measuring the ferrite content and using guidelines or an embrittlement model to determine if the ferrite value is acceptably low. The third technique is to measure the current Charpy V-notch impact energy, fracture toughness, or microhardness of samples that have been removed from a component; then the first technique, i.e; the simplified analytical model, is used to estimate the J_{Ic} value at EONOP.

In the sixth step, the minimum required fracture toughness from Step 4 is compared with the estimated actual lower-bound fracture toughness at EONOP from Step 5, and the margin of safety is determined. Using the estimated stresses from Step 4 and the estimated lower-bound toughness from Step 5, critical crack size is determined. Then, the detectability of the critical flaw size is assessed. Finally a leak-before-break (LBB) analysis is performed to determine the margin between the critical crack length and the leakage-detectable crack length that corresponds to ten times the detectable leak rate.

Once the component integrity at EONOP is evaluated, a plan of action is developed in the seventh step. If acceptable safety margins are present, and the ASME Section III cumulative fatigue usage factor at EONOP is less than 1.0, continued operation to EONOP may be permitted. Potential need for repair or replacement must be considered.

The eighth step is to establish a plan for future ISI of the component. The plan should define both the extent of inspection required and the interval at which reinspection should be performed. It may be useful to consider developing a thermal-embrittlement surveillance program similar to the programs used for evaluating radiation effects. Such a program would provide valuable data from realistic exposure conditions.

The ninth step is to reevaluate the component after future inspections or as required by other circumstances. The reevaluation will start at Step 2, upgraded by the data from the most recent evaluation, and will proceed from that point.

The major difficulties in implementing this overall procedure are encountered in Step 5, Assess Component Condition. The simplified analytical model (Step 5.1) can be applied with a reasonable degree of confidence, even though further validation of the correlation between CVN and J_{Ic} values is needed (see Figures 12 and 14). However, ferrite assessment (Step 5.2) and the measurement of properties (Step 5.3) have not been fully developed and validated. Quantitative evaluations of possible ferrite measurement techniques and subsized specimen testing methods are needed. Correlations and/or models are needed to relate ferrite content, spacing, and hardness to the amount of thermal embrittlement. Also, a model for predicting future degradation caused by thermal embrittlement should be developed to remove uncertainties associated with the current approach. Thus, considerable work is needed in the area of assessing and forecasting the condition of cast stainless steel components that operate at temperatures near 300°C (570°F) in light water reactors.

Fracture-mechanics evaluations also could be difficult to conduct in some situations. Framatome has performed fracture mechanics evaluations for their cast stainless steel components and has developed a minimum required value of 100 kJ/m^2 for J_{Ic} at the end of operating life.[a] The establishment of a minimum J_{Ic} value simplifies the evaluation of standardized components because there is no need to repeat the fracture-mechanics analysis for each case. However, such a simplified approach may not be applicable to all U.S. LWRs because of the variation in component design, fabrication, and operation from one reactor to another. It would be useful to perform fracture-mechanics analyses for several different classes of cast stainless steel components, so minimum required values of J_{Ic} at the end of operating life could be developed for each class. These values then could be applied to the case-by-case evaluation of components for license renewal.

a. Unpublished paper presented by G. Slama et al., at SMiRT Postconference Seminar 6 at Monterey, California, August 29-30, 1983.

7. SUMMARY

This report has reviewed the quantification of thermal embrittlement damage in CF–8, CF–8M, and CF–3 cast stainless steel components subjected to light water reactor (LWR) operating temperatures. These alloys have an austenite matrix with islands of ferrite. For LWR applications, typical volume fractions of the ferrite phase are in the range of 8 to 20%. The ferrite phase is subject to embrittlement by the formation of alpha–prime after long–term (many years) exposures at temperatures near 300°C (570°F). The amount, distribution, and degree of embrittlement of the ferrite phase determine the extent to which a component has been degraded by thermal embrittlement. This degradation is manifested by a loss of Charpy V–notch (CVN) impact energy and fracture toughness (J_{Ic}). Other mechanical properties, such as tensile strength, fatigue strength, and low–cycle fatigue–crack–growth resistance are not markedly affected by thermal embrittlement, so the primary concern in addressing the renewal or extension of LWR operating licenses is the loss of fracture toughness after long–term service. However, more data on the effect of thermal embrittlement on fatigue–crack–growth resistance are needed, especially for CF–8 stainless steel and for high–cycle fatigue.

From the maximum service temperature and chemical composition of the alloy, an aging parameter is proposed for estimating the lower–bound room–temperature CVN values for service times up to 100 years, or the minimum CVN values at a very long time can be estimated using the Φ parameter. A CVN impact energy versus J_{Ic} correlation then can be used to estimate a corresponding lower–bound value of the fracture toughness.

Nondestructive examination (NDE) of cast stainless steel components yields information on the size, location, and distribution of defects. This information can be employed in fracture–mechanics evaluations of structural integrity. However, because of the coarse and variable nature of the microstructure of cast stainless steels, ultrasonic testing (UT) is limited in its usefulness as an NDE tool; radiography normally is used for the NDE of these materials, especially for thick sections. Research is in progress to develop and validate advanced UT methods for inservice inspection of cast stainless steel components. However, neither current nor advanced NDE methods characterize the mechanical properties or metallurgical condition (degree of embrittlement) of inservice components.

Correlations have been developed for estimating the ferrite content of stainless steel castings from their chemical composition. However, these correlations do not predict the ferrite spacing, which is a parameter that influences fracture toughness. Castings that contain more than about 10 to 15% ferrite appear to be the most susceptible to thermal embrittlement, but no precise guideline for an acceptable ferrite content has been established, and material with even less than 10% ferrite may be degraded by thermal embrittlement. Metallographic examination of small samples removed from components or of surface replicas can provide data on the ferrite content and spacing at specific locations in castings. The ferritescope is a magnetic instrument that can be used in the field to nondestructively measure ferrite contents up to 30%.

Subsized specimens from small samples of material that have been removed from service can be used to measure fracture toughness. Guidelines for minimum specimen size are provided by ASTM E 813. Those guidelines are expected to be conservative, but they have not been verified directly for the testing of cast stainless steels.

Long–term service exposure increases the microhardness in the ferrite phase of cast stainless steels, but no correlation between the measured microhardness and change in impact resistance or fracture toughness has been established. The correlation also would have to account for the effects of ferrite content and spacing to provide a quantitative estimate of fracture toughness.

Weld–repair procedures have been developed for the removal of casting defects during original fabrication. It should be reasonably easy to adapt these procedures to the inservice repair of stainless steel castings. However, repair welding has not been fully qualified and validated for material that has been thermally embrittled by long–term service exposures in LWR environments.

The recommended approach for evaluating cast stainless steel components for LWR license renewals, is to assess the current condition of the component, estimate its remaining safe life, and decide on continued as–is use, repair, or replacement of the component. The

alternative approach of automatically replacing a component after a given period of service is not usually feasible.

A nine-step procedure for the aging and license renewal evaluation of cast stainless steel components has been outlined. The first three steps include the review of fabrication and construction records, ISI records, and operating history of the components. In the fourth step, the data collected from these reviews are used to perform the fracture mechanics evaluation to determine the minimum required fracture toughness and the worst-flaw size at the end of the extended operating period (EONOP). Three different methods are presented in Step 5 to estimate the lower-bound fracture toughness of cast stainless steel components at EONOP. Then, the minimum required fracture toughness at EONOP is compared with the corresponding estimated lower-bound value, and a leak-before-break analysis is performed. The action regarding continued operation, repair, or replacement of a component is established in Step 7, and finally, plans for the next ISI are made.

8. RECOMMENDED FUTURE WORK

Improved methods need to be developed for evaluating the fitness of cast stainless steel LWR components for service during original or extended licensing periods and for reducing the conservatism inherent in the procedures discussed above. Therefore, we recommend that future work be undertaken in the following 13 areas:

1. Guidelines of worst-case data should be developed for use when case-specific data are not available.

2. Thermal-embrittlement surveillance programs similar to the programs used for evaluating radiation effects should be developed. Such programs would provide valuable data from realistic exposure conditions.

3. More CVN and J_{Ic} data on thermally aged material tested at normal LWR operating temperatures [about 280 to 290°C (536 to 554°F)] are needed.

4. An improved aging parameter should be developed that more accurately models the aging mechanisms that cause thermal embrittlement during long-term service exposures.

5. Work should be undertaken to determine if there is some critical combination of ferrite level and spacing above which ferrite distribution in cast stainless steel is continuous. If such a limit exists, then a method of estimating ferrite content and spacing from composition and production history should be developed.

6. Fatigue-crack-growth studies of aged CF-8 stainless steel should be performed. Near-threshold, as well as low-cycle, tests are needed on both aged and irradiated materials. Data for high-cycle fatigue behavior of aged CF-8M stainless steel are also needed.

7. The use of metallographic surface replication, the ferritescope, and other magnetic-property measurement tools, along with eddy-current methods, should be evaluated, demonstrated, and validated as inservice NDE tools for evaluating the condition of stainless steel castings.

8. Experimental studies should be performed to determine the smallest specimen size for valid measurement of the fracture toughness of cast stainless steels.

9. Work should be undertaken to evaluate the correlation between the microhardness of the ferrite phase and fracture toughness for cast stainless steels.

10. Procedures for repair welding cast stainless steels that have been subject to long-term service in LWR environments should be qualified and validated for use in license renewal.

11. Fracture-mechanics analyses of representative component/load-history combinations should be conducted. Such analyses can provide estimates of the required minimum J_{Ic} value.

12. Current work on the development of advanced ultrasonic methods for inspection of cast stainless steel components should be continued.

13. Present ISI programs should be modified to obtain essential data that are needed for the evaluation of LWR cast stainless steel components.

9. REFERENCES

Alexander, D. J., et al. (1990). "The Effect of Aging at 343°C on Type 308 Stainless Steel Weldments," *Fatigue, Degradation, and Fracture—1990, ASME PVP–Vol. 195, MCP–Vol.30*, New York, presented at *the 1990 Pressure Vessels and Piping Conference, Nashville, Tennessee, June 17–21, 1990*, pp. 187–192.

ASTM (1986). *The Use of Small–Scale Specimens for Testing Irradiated Material*, ASTM STP 888, Philadelphia.

Aubrey, L. S., et al. (1982). "Ferrite Measurement and Control in Cast Duplex Stainless Steels," *Stainless Steel Castings*, ASTM STP 756, The American Society for Testing and Materials, Philadelphia, pp. 126–164.

Auerkari, P. (1983). "Remnant Creep Life Estimation of Old Power Plant Steam Piping Systems," *Advances in Life Prediction Methods*, The American Society of Mechanical Engineers, New York, pp. 353–356.

Auger, P., et al. (1990). "Atom probe and transmission electron microscopy study of aging of cast duplex stainless steels." *Materials Science and Technology, 6*, pp. 301–313.

Avioli, Jr., M. J. (1986). "Application of Advanced UT Systems to the Preservice Inspection of Centrifugally Cast Stainless Steel Pipes in Power Plants," *Nondestructive Evaluation Program: Progress in 1985*, EPRI NP–4315–SR, pp. 6–1 to 6–8.

Bamford, W. H., et al. (1985). "Thermal Aging of Cast Stainless Steel, and Its Impact on Piping Integrity," *Journal of Engineering Materials and Technology, 107*, 1, pp. 53–60.

Bamford, W. H., et al. (1987). "Aging Effects on Cast Stainless Steels," *Properties of Stainless Steels in Elevated Temperature Service*, MPC–Vol. 26, PVP–Vol. 132, The American Society of Mechanical Engineers, New York, pp. 49–63.

Bonnet, S., et al. (1990). "Relationship between evolution of mechanical properties of various cast stainless steels and metallurgical and aging parameters; outline of current EDF programmes," *Materials and Science Technology, 6*, pp. 221–229.

Brown, J. E., et al. (1990). "The Thermal Aging of Alloys Modelling the Ferrite Phase in Stainless Steel Castings," *Fatigue, Degradation, and Fracture—1990, PVP–Vol. 30*, The American Society of Mechanical Engineers, New York, pp. 175–185.

Buchalet, C., Y. Meyzaud, and Ph. Taupin (1985). "Effect of Long–Term Aging on the Critical Defect Sizes in Primary Piping Cast Stainless Steel Elbows," *Proceedings of the Second International Conference on Environmental Degradation of Materials in Nuclear Power Systems—Water Reactors, Monterey, California, September 9–12, 1985*, ANS/TMS–AIME/NACE, pp. 477–484.

Chopra, O. K. (1990). "Thermal Aging of Cast Stainless Steels: Mechanisms and Predictions," *Fatigue, Degradation, and Fracture—1990, PVP–Vol. 195, MPC–Vol. 30*, The American Society of Mechanical Engineers, New York, pp. 193–214.

Chopra, O. K., and H. M. Chung (1985). "Aging of Cast Duplex Stainless Steels in LWR Systems," *Nuclear Engineering and Design, 89*, pp. 305–318.

Chopra, O. K., and H. M. Chung (1986a). "Aging of Cast Stainless Steel," *Thirteenth Water Reactor Safety Research Information Meeting*, 2, NUREG/CP–0072, pp. 387–407.

Chopra, O. K., and H. M. Chung (1986b). "Investigations of the Mechanisms of Thermal Aging of Cast Stainless Steels," presented at the *Metal Component Subcommittee of the Advisory Committee on Reactor Safeguards Meeting, Columbus, Ohio, July 1–2, 1986*, transcript available from NRC Public Document Room.

Chopra, O. K., and H. M. Chung (1986c). *Long-Term Embrittlement of Cast Duplex Stainless Steels in LWR Systems: Semiannual Report October 1985–March 1986*, NUREG/CR-4744 Vol. 1, No. 1, ANL-86-54.

Chopra, O. K., and H. M. Chung (1987). *Long-Term Embrittlement of Cast Duplex Stainless Steels in LWR Systems: Semiannual Report April–September 1986*, NUREG/CR-4744 Vol. 1, No. 2, ANL-87-16.

Chopra, O. K., and H. M. Chung (1989a). "Aging of Cast Stainless Steels," presented by W. Shack at *ACRS Metal Components Subcommittee Meeting, Battelle, Columbus, Ohio*, March 15, 1989, transcript available from NRC Public Document Room.

Chopra, O. K., and H. M. Chung (1989b). "Initial Assessment of the Processes and Significance of Thermal Aging in Cast Stainless Steels," *Sixteenth Water Reactor Safety Information Meeting, National Institute of Standards and Technology, Gaithersburg, Maryland, October 24–27, 1988*, NUREG/CP-097, Vol. 3, pp. 519–546.

Chopra, O. K., and H. M. Chung (1990a). "Cast Stainless Steel: Mechanisms and Predictions," *Transactions of the 17th Water Reactor Safety Research Information Meeting*, Rockville, Maryland, October 23–25, 1989, NUREG/CP-0105, Vol. 3, pp. 319–344.

Chopra, O. K., and H. M. Chung (1990b). "Long-Term Embrittlement of Cast Duplex Stainless Steels in LWR Systems: Semiannual Report October 1987–March 1988," NUREG/CR-4744 Vol. 3, No. 1, ANL-89/22.

Chopra, O. K., and A. Sather (1990). "Initial Assessment of the Mechanisms and Significance of Low-Temperature Embrittlement of Cast Stainless Steels in LWR Systems," NUREG/CR-5385, ANL-89/17.

Chung, H. M. (1989). "Thermal Aging of Decommissioned Reactor Cast Stainless Steel Components and Methodology for Life Predictions," *Life Assessment and Life Extensions of Power Plant Components—1989: Presented at the 1989 ASME Pressure Vessels and Piping Conference—ASME Co-sponsorship*, Honolulu, Hawaii, July 23–127, 1989, p. 111.

Copeland, J. F., and A. J. Giannuzzi (1984). *Long-Term Integrity of Nuclear Power Plant Components*, EPRI-NP-3673-LD, October.

Corwin, W. R., and A. M. Hougland (1986). "Effect of Specimen Size and Material Condition on the Charpy Impact Properties of 9Cr-1Mo-V-Nb Steel," *The Use of Small-Scale Specimens for Testing Irradiated Material*, ASTM STP 888, The American Society for Testing and Materials, Philadelphia, pp. 325–338.

Curtis, G. C., and J. Sherwin (1961). "Magnetic method for the estimation of ferrite in stainless steel welds," *British Journal of Applied Physics*, 12, pp. 344–345.

Devine, T. M. (1980), "Influence of Carbon Content and Ferrite Morphology on the Sensitization of Duplex Stainless Steel," *American Society for Metals, Metallurgical Transaction* A, 11A, May, pp. 791–800.

Dombret, P., P. Caussin, and P. Rorive (1990), "Developing Ultrasonics for PWR Pump Bowl Inservice Inspection," *Nuclear Engineering International*, pp. 42–44.

Egan, G. R., et al. (1987). *Inspection of Centrifugally Cast Stainless Steel Components in PWRs*, EPRI NP-51 31.

EPRI (1986). "Inspection of PWR Cast Pipes," *EPRI Journal*, *11*, 5, pp. 57–58.

Georgetown University (1988). *Lamb Wave Inspection for Large Cracks in Centrifugally Cast Stainless Steel*, EPRI NP-5963.

Greenstreet, W. L., et al. (1985). *Aging and Service Wear of Check Valves Used in Engineered Safety-Feature Systems of Nuclear Power Plants*, NUREG/CR-4302, Vol. 1, ORNL-6193/V1, p. 9.

Gregory, M. C., et al. (1986). "Ultrasonic Characterization of Centrifugally Cast Stainless Steel Samples," *Nondestructive Evaluation Program: Progress in 1985*, EPRI NP-4315-SR, pp. 3–1 to 3–12.

Haggag, F. M., et al. (1985). "The Use of Miniaturized Tests to Predict Flow Properties and Estimate Fracture Toughness in Deformed Steel Plates," *International Conference and Exhibition on Fatigue, Corrosion Cracking, Fracture Mechanics, and Failure Analysis, Salt Lake City, Utah, December 1985.*

Harth, G. H., and T. P. Sherlock (1985). "Monitoring the Service Induced Damage in Utility Boiler Pressure Vessels and Piping Systems," *Residual-Life Assessment, Nondestructive Examination, and Nuclear Heat Exchanger Materials*, PVP-Vol. 98-1, The American Society of Mechanical Engineers, New York, pp. 19-23.

Hazelton, W. S., and W. H. Koo (1988). *Technical Report on Material Selection and Processing Guidelines for BWR Coolant Pressure Boundary Piping*, NUREG-0313, Rev. 2.

Henry, J. F., and F. V. Ellis (1983). *Plastic Replication Procedures for Damage Assessment*, progress report on EPRI Project RP2253-1.

Hertzberg, R. W. (1983). *Fracture Mechanics of Engineering Materials*, Second Edition, New York: John Wiley & Sons, p. 470.

Hilton, S. O., and M. F. Steakley (1986). "Steam Line Inspection Program for Tennessee Valley Authority's High Temperature Steam Piping Systems," *EPRI Conference on Life Extension and Assessment of Fossil Plants, Washington, D.C., June 1986.*

Hiser, A. L. (1987). "Tensile and J-R Curve Characterization of Thermally Aged Austenitic Cast Stainless Steel," *Properties of Stainless Steels in Elevated Temperature Service*, MPC-Vol. 26, PVP-Vol. 132, The American Society of Mechanical Engineers, New York, 1987, pp. 35-48. (Also, see NUREG/CR-5024, 1988.)

Huang, F. H. (1986). "Use of Subsized Specimens for Evaluating the Fracture Toughness of Irradiated Materials," *The Use of Small-Scale Specimens for Testing Irradiated Material*, ASTM STP 888, Philadelphia, pp. 290-304.

Hughes, N. R., W. L. Clarke, and D. E. Delwiche (1982), "Intergranular Stress-Corrosion Cracking Resistance of Austenitic Stainless Steel Castings," *Stainless Steel Castings*, ASTM STP, V. G. Behal and A. S. Melilli (eds.), pp. 26-47.

Janiszewski, J. A., et al. (1986). "A Production Approach to On-Site Metallographic Analysis," *EPRI Conference on Life Extension and Assessment of Fossil Plants, Washington, D.C., June 1986.*

Jaske, C. E., et al. (1986). "Life-Assessment of High-Temperature, Fossil-Plant Components," *EPRI Conference on Life Extension and Assessment of Fossil Plants, Washington, D.C., June 1986.*

Jeong, P., and F. Ammirato (1989). *Ultrasonic Examination of Cast Stainless Steel*, EPRI-NP-6299.

Kupperman, D. S., K. J. Reimann, and J. Abrego-Lopez (1987), "Ultrasonic NDE of Cast Stainless Steel," *NDT International, 20*, 3, pp. 145-152.

Landerman, E. I., and W. H. Bamford (1978). "Fracture Toughness and Fatigue Characteristics of Centrifugally Cast Type 316 Stainless Steel Pipe After Simulated Thermal Service Conditions," *Ductility and Toughness Considerations in Elevated Temperature Service*, MPC-8, The American Society of Mechanical Engineers, New York, 1978, pp. 99-127.

Leger, M. T. (1982). "Predicting and Evaluating Ferrite Content in Austenitic *Stainless Steel Castings*," Stainless Steel Castings, ASTM STP 756, The American Society for Testing and Materials, Philadelphia, pp. 105-125.

Lucas, G. E., et al. (1986). "Subsized Bend and Charpy V-Notch Specimens for Irradiated Testing," *The Use of Small-Scale Specimens for Testing Irradiated Material*, ASTM STP 888, Philadelphia, pp. 305-324.

Manahan, M. P., et al. (1981). "The Development of a Miniaturized Disc Bend Test for Determination of Post Irradiation Mechanical Properties," *Journal of Nuclear Materials, 103-104*, pp. 1545-1550.

Masuyama, F., et al. (1985). "Findings on Creep–Fatigue Damage in Pressure Parts of Long–Term Service–Exposed Thermal Power Plants," *Journal of Pressure Vessel Technology, 107*, pp. 260–270.

McConnell, P., et al. (1986). "Experience in Subsized Specimen Testing," *The Use of Small–Scale Specimens for Testing Irradiated Material*, ASTM STP 888, Philadelphia, pp. 353–368.

Mills, W. J. (1987). "Fracture Toughness of Aged Stainless Steel Primary Piping and Reactor Vessel Materials," *Journal of Pressure Vessel Technology, 109*, November, pp. 440–448.

Misawa, T., and Y, Hamaguchi (1986). "Miniature Specimen Tests for Evaluating Fracture Resistance With Radiation and Hydrogen Embrittlements in Ferritic Steel," *The Mechanism of Fracture*, American Society for Metals, Metals Park, Ohio, pp. 521–527.

Neubauer, B., and U. Wedel (1983). "Restlife Estimation of Creeping Components by Means of Replicas," *Advances in Life Prediction Methods*, The American Society of Mechanical Engineers, New York, pp. 307–313.

Padden, T. R. (1983). *Metallurgical Characterization of the Creep Ratcheting Test Article Failure*, WAESD–HT–94000–28, Westinghouse Electric Corporation, Madison, Pennsylvania.

Padden, T. R., and C. A. Daniels (1976). *In Situ Examination of the Small Scale Steam Generator Model*, WARD–I10134–1, Westinghouse Electric Corporation, Madison, Pennsylvania.

Padden, T. R, and C. A. Daniels (1981). "Replication Manipulator and Procedure for Tube Bore Surfaces," presented at the *Annual Meeting of Scanning Electron Microscopy, Inc., Dallas, Texas, April 1981.*

Peckner, D., and I. M. Bernstein (1977). *Handbook of Stainless Steels*, New York: McGraw–Hill Book Company.

Reed–Hill, R. E. (1973). *Physical Metallurgy Principles*, second edition, New York: D. Van Nostrand Company, pp. 568–610.

Sassen, J. M., et al. (1987). "Kinetics of Spinodal Decomposition in the Ferrite Phase of a Duplex Stainless Steel," *Properties of Stainless Steels in Elevated Temperature Service*, MPC–Vol. 26, PVP–Vol. 132, The American Society of Mechanical Engineers, New York, pp. 65–78.

Shah, V. N., and P. E. MacDonald (eds.), (1987). *Residual Life Assessment of Major Light Water Reactor Components—Overview*, Vol. 1, NUREG/CR–4731, EGG–2469, p. 66.

Shah, V. N., and P. E. MacDonald (eds.), (1989). *Residual Life Assessment of Major Light Water Reactor Components—Overview*, Vol. 2, NUREG/CR–4731, EGG–2469.

Shankar, R., G. Selby, and P. Jeong (1988). "Defect Detection and Signal Processing for Cast Stainless Steel," *International Journal of Pressure Vessel & Piping, 35*, pp. 57–71.

Solomon, H. D., and T. M. Devine, Jr. (1983). "Keynote Address: A Tale of Two Phases," *Duplex Stainless Steels* (Conference Proceedings of the American Society for Metals), R. A. Lula (ed.), Metals Park, Ohio 44073: American Society for Metals, pp. 693–756.

Swanson, G. D. (1981). *Development of Fracture Toughness Measurement Capability by Ultrasound*, Final Report BDX–613–2625, Bendix, Kansas City Division.

Takigawa, T., et al. (1986). "Life Assessment and Extension of Steam Turbine Rotor – Overview of MHI's Activities," *EPRI Conference on Life Extension and Assessment of Fossil Plants, Washington, D. C., June, 1986.*

Trautwein, A., and W. Gysel (1982). "Influence of Long–Time Aging of CF8 and CF8M Cast Steel at Temperatures Between 300 and 500°C on Impact Toughness and Structural Properties," *Stainless Steel Castings*, ASTM STP 756, Philadelphia, pp. 165–189.

Umino, D. T., and A. K. Rao (1984). *Long-Term Inspection Requirements for PWR Pump Casings*, EPRI NP-3491.

USNRC (1978). "Control of Ferrite Content in Stainless Steel Weld Metal," *Regulatory Guide 1.31*, Revision 3.

USNRC (1988a). *Licensed Operating Reactors Status Summary Report Data as of 05-31-88*, NUREG-0020, Vol. 12, No. 6.

USNRC (1988b). Office of Nuclear Reactor Regulation, *Thermal Stresses In Piping Connected To Reactor Coolant Systems*, NRC Bulletin No. 88-08, Supplement 2, August 4.

Vary, A. (1976). "The Feasibility of Ranking Material Fracture Toughness by Ultrasonic Attenuation Measurements," *Journal of Testing and Evaluation*, *4*, 4, pp. 251-256.

Viswanathan, R. (1985). "Dissimilar Metal Weld and Boiler Creep Damage Evaluation for Plant Life Extension," *Residual-Life Assessment, Nondestructive Examination, and Nuclear Heat Exchanger Materials*, PVP-Vol. 98-1, The American Society of Mechanical Engineers, New York, pp. 9-18.

NRC FORM 335 (2-89) NRCM 1102 3201, 3202

U.S. NUCLEAR REGULATORY COMMISSION

BIBLIOGRAPHIC DATA SHEET

(See instructions on the reverse)

1. REPORT NUMBER (Assigned by NRC. Add Vol., Supp., Rev., and Addendum Numbers, if any.)
NUREG/CR-5314, Vol. 3
EGG-2562

2. TITLE AND SUBTITLE

Life Assessment Procedures for Major LWR Components

Cast Stainless Steel Components

3. DATE REPORT PUBLISHED
MONTH: October
YEAR: 1990

4. FIN OR GRANT NUMBER
A6389

5. AUTHOR(S)

C.E. Jaske, V.N. Shah

6. TYPE OF REPORT
Technical

7. PERIOD COVERED *(Inclusive Dates)*

8. PERFORMING ORGANIZATION — NAME AND ADDRESS *(If NRC, provide Division, Office or Region, U.S. Nuclear Regulatory Commission, and mailing address; if contractor, provide name and mailing address.)*

Idaho National Engineering Laboratory
EG&G Idaho, Inc.
Idaho Falls, Idaho 83415

9. SPONSORING ORGANIZATION — NAME AND ADDRESS *(If NRC, type "Same as above"; if contractor, provide NRC Division, Office or Region, U.S. Nuclear Regulatory Commission, and mailing address.)*

Division of Engineering
Office of Nuclear Regulatory Research
U.S. Nuclear Regulatory Commission
Washington, DC 20555

10. SUPPLEMENTARY NOTES

13. ABSTRACT (200 words or less)

This report presents a procedure for estimating the current condition and residual life of safety-related cast stainless steel components in light water reactors (LWRs). The procedure accounts for loss of fractures toughness caused by thermal embrittlement and includes the following: a review of design and fabrication records, inservice inspection records, and operating history; a fracture mechanics evaluation to determine the required toughness estimates; and criteria regarding continued service, repair, or replacement of the component being evaluated. The report discusses the available Charpy V-notch impact energy, fracture toughness, tensile strength, fatigue resistance, and fatigue-crack growth data, and presents two methods for assessing the degree of thermal embrittlement: metallurgical evaluation and analytical modeling of inservice degradation.

12. KEY WORDS/DESCRIPTORS *(List words or phrases that will assist researchers in locating the report.)*

LWR cast stainless steel components
Thermal embrittlement
Charpy impact energy
Fracture toughness
Life assessment procedure
Inservice inspections
Fatigue

13. AVAILABILITY STATEMENT
unlimited

14. SECURITY CLASSIFICATION
(This Page) unclassified
(This Report) unclassified

15. NUMBER OF PAGES

16. PRICE